EXPERIMENTAL VERIFICATION
OF
THEODORSEN'S THEORETICAL
JET BOUNDARY CORRECTION FACTORS

A THESIS

SUBMITTED FOR THE DEGREE

OF

MASTER OF SCIENCE IN AERONAUTICAL ENGINEERING

BY

GEORGE VAN SCHLIESTETT

Atlanta, Georgia.
Daniel Guggenheim School of Aeronautics
Georgia School of Technology
May 11, 1934

A/N Sgt 34

35961

Approved:

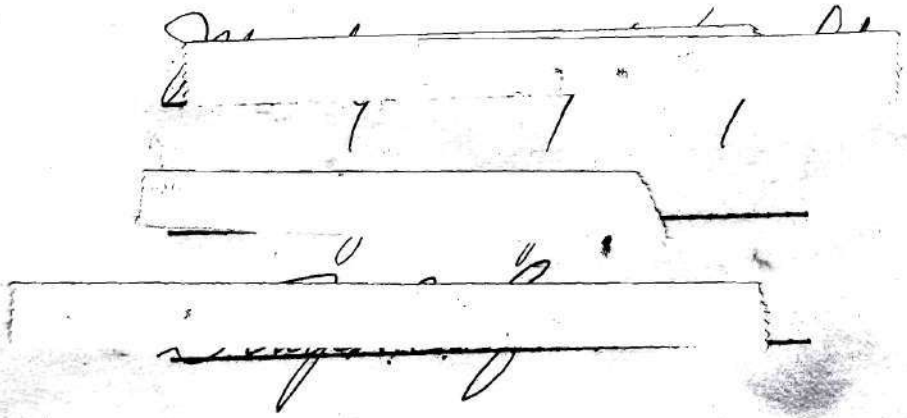

EXPERIMENTAL VERIFICATION OF THEODORSEN'S THEORETICAL JET BOUNDARY CORRECTION FACTORS

Introduction

The pioneer work on tunnel wall interference for circular tunnels is due to L. Prandtl, Director of the Gottingen Aeronautics Laboratory. In his classic " Applications of Modern Hydrodynamics to Aeronautics" (Ref.1) he points out that due to the limited cross-section area of the wind tunnel airstream, the deflection of the air behind a model is larger or smaller than it would be in free air depending on whether the boundary is open or closed. To account for this deflection or " downwash" he introduced imaginary vortices (Fig.a) so placed with respect to the tunnel as to satisfy

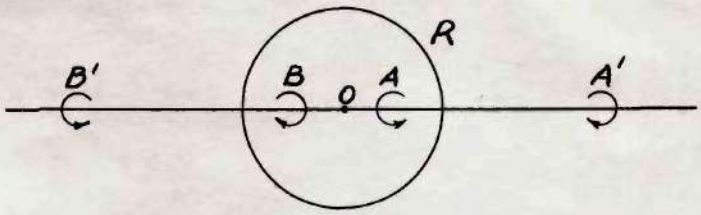

Fig. a

the condition of the boundary at the test section; i.e., zero velocity normal to the boundary of the closed tunnel, or, in the case of the open jet, the same pressure at the surface of the jet as in the surrounding quiet air. The problem then resolved into determining the velocity at the center of the tunnel induced by the imaginary vortices. The result is found to be as follows in the closed tunnel

$$w = \frac{C_L S V}{8\pi R^2} \cdot$$

Hence the upward inclination of the airstream due to the

interference of the boundary becomes

$$\epsilon_1 = \frac{w}{V} = \frac{1}{8}\frac{S}{C}C_L \text{ , where } C = \pi R^2$$

Then the corrections take the form

$$\Delta\alpha = \delta\frac{S}{C}C_L,$$

$$\Delta C_D = \delta\frac{S}{C}C_L^2$$

in which the correction factors are

δ = .125 for the closed circular tunnel

δ =-.125 for the open circular tunnel.

Prandtl suggested that the interference of walls of rectangular section could be found by arranging an infinite number of imaginary tunnels around the original in such a manner as to satisfy the required boundary conditions.

Working along the line of this suggestion, H. Glauert, of Trinity College, Cambridge, contributed his development of the theory for interference of closed rectangular tunnels (Ref.2). He determined the velocity at the center of the tunnel due to the image system satisfying the condition of the vertical boundaries alone, to which he added the effect of the system satisfying the condition of the horizontal boundaries.

Computation by his theory gives the following table:

Correction factors for closed rectangular tunnels of width to height ratio b/h

b/h	1/4	1/2	1	$\sqrt{2}$	2	4
δ	.524	.262	.137	.119	.137	.262

In 1931, Theodore Theodorsen, physicist for the National Advisory Committee for Aeronautics, presented a paper "devoted to a systematic analytical treatment of the properties and relative advantages of the several possible arrangements of rectangular tunnels, including the conventional types." (Ref.3) His method of summation of the induced velocities differs from that used by Glauert, but his numerical results for the closed tunnel are the same. Compare the following table with the one preceding.

Correction factors for closed rectangular tunnels of width to height ratio b/h

b/h	1/4	1/2	1	$\sqrt{2}$	2	4
δ	.523	.263	.138	.120	.137	.262

Theory indicates that there are only three boundary arrangements for rectangular tunnels that cause no deflection of the airstream. (See Fig.1) Excepting these, all tunnels require boundary interference corrections. At present, experimental verification of theory is available for only circular tunnels and some rectangular tunnels.

It is the purpose of this report to provide experimental verification of Theodorsen's theoretical corrections for the square tunnel with five boundary types. The following designations of types are his:

Case I - Closed tunnel.

Case II - Free jet.

Case III - Jet with horizontal boundaries.

Case IV - Jet with vertical boundaries.

Case V - Jet with one horizontal boundary.

In addition, tests were made to find out whether a boundary of " slots and slats" of equal width and parallel to the horizontal center line would give zero correction - the average of the open and closed tunnels with square jet.

Method of Test

Force tests were made on an airfoil model 3" x 18" (span 60 percent of width of tunnel) at an airspeed of seventy-five miles per hour. In addition, a model 3" x 12" (span 40 percent of width of tunnel) was tested for Cases I, II, and VI (slots and slats) to observe the effect of span on the deflection of the stream.

The tunnel has a two and one-half foot square open jet (Fig.2), maximum airspeed of 105 m.p.h., and maximum variation in dynamic pressure less than one percent in the region occupied by the wing.

The forces were measured by means of the six-component wire balance system shown in Fig.3. The lift is measured directly on the large balance as the sum of the forces sustained by the two lift wires. The drag is applied to the horizontal wire along the center line of the tunnel, from which it is transmitted to the vertical wire, which is attached to the drag balance. The forces on the wires are made equal by the effect of a 45° wire at their

juncture. The pitching moment is the product of the force on the downstream lift wire and the distance to the other lift wire. The yawing moment is the product of the cross wind force on the downstream horizontal wire and the distance between the lift wires. The rolling moment is the product of the lower front cross wind component and its distance from the center line of the tunnel. The algebraic sum of the three cross wind components is the cross wind force. In this report only lift and drag are considered.

The various boundaries were set up by bolting walls around the jet. The closed jet is shown in Fig.4. The slots and slats (Fig.5) are each 1-1/2" wide. In this figure, which the author designates as Case VI (a), the horizontal center line of the side walls is along a "slot". Case VI (b) is arranged by dropping the side walls 1-1/2" until the horizontal center line is along a "slat".

The two wings, 3"x 18" and 3" x 12", were made of laminated mahogany, shaped to a Clark Y section with a tolerance of $\pm$ .003". The large wing had a twist of 0.5°, producing an error in the correction factor δ_D amounting to 0.041 at C_L = 0.1, but rapidly decreasing to 0.002 at C_L = 0.6. A twist of 0.3° in the smaller wing caused errors of 0.021 at C_L = 0.1 and 0.001 at C_L = 0.6. However, these errors had negligible effect on the results, since correction factors near zero lift were

not included in the average.

As to precision of measurements, unusual care was observed in reading the balances, since the results depended on the accuracy of determining small differences between relatively large quantities. Then to reduce probability of a constant error due to misreading the static tare, this reading was checked after each run. By making two runs for each set-up, the error in individual force measurements was averaged out. The upward inclination of the airstream ($\epsilon = .4^{\circ}\pm$) was accounted for by averaging the results of tests in the normal and inverted positions(Fig.6).

It was found that the dynamic tare of the frame varied with the angle of attack of the airfoil (Fig.7,(a),(b),). This tare was found by supporting a dummy wing in the same position relative to the frame as the real wing had occupied, but not attached to the frame. The dummy wing was moved through the range of angle of attack of the real wing and the tare of the frame and wires observed.

The error in average readings was less than one percent, but the drag was two percent too high near zero lift, probably due to interference of the frame on the wing which was not accounted for by the method of finding the interference induced on the frame by the wing.

Results

Although the dynamic pressure variation in the region occupied by the model was in all cases less than one percent, the mean value was found by integrating dynamic pressure readings observed at intervals across the airfoil span for each jet type. Test results were calculated on the basis of the mean value. These are presented in non-dimensional form in Tables I to VII and Figures 8 to 10.

The following equations were used in reducing the test data to coefficient form:

$$C_L = \frac{L}{qS}$$

$$C_D' = \frac{D'}{qS}$$

$$\alpha' = \alpha_g - \alpha_{L_0}$$

where

C_L = absolute lift coefficient

C_D' = absolute drag coefficient with preliminary corrections, not including jet boundary effect.

C_D = absolute drag coefficient corrected for jet boundary effect.

α' = angle of attack in degrees measured from zero lift.

α = angle of attack measured from zero lift and corrected for jet boundary effect.

α_g = geometric angle of attack measured with respect to the chord line.

α_{L_o} = geometric angle of attack of zero lift.

L = measured lift.

D' = measured drag with preliminary corrections, not including jet boundary effect.

q = mean dynamic pressure over span of model.

S = area of airfoil.

The preliminary corrections for temperature - alcohol density variations of the manometer were made with the aid of a chart (Ref.5). The average drag coefficients at zero lift were 0.0239 and 0.0259 for the airfoils of aspect ratios 6 and 4 respectively. The several drag curves were shifted so that they all had the same minimum drag corresponding to the respective aspect ratios.

The test results mentioned in this report are net quantities, the tare of the frame having been subtracted.

The effect of turbulence was not considered in these tests.

The next step was the application of the theoretical jet boundary corrections. These are of the form:

$$\Delta\alpha = \delta \frac{S}{C} c_L \quad \text{(in radians)}$$

$$= \delta \frac{S}{C} c_L \frac{180}{\pi} \quad \text{(in degrees)}$$

$$\Delta c_D = \delta \frac{S}{C} c_L^2$$

where S = area of airfoil.

C = cross-sectional area of the jet.

δ = correction factor from Table VIII

(which is Table I in Ref.3)

The drag curves first obtained after application of the theoretical correction factors showed Cases IV and V to have large divergence from the other Cases. The test method was checked, but no possibilities for such large errors could be found. Then the theory was studied again and analyzed with the view to accounting for these discrepancies. The sources of the errors were discovered and eliminated as described later in the discussion. The new factors were applied to get the correct drag and angle of attack presented in Tables I to VII and Figures 11 to 13.

The drag in Case III diverged slightly from the others, but no error in the theory could be found. This matter will be left for the chapter " Analysis of Results".

The results of the test with one horizontal boundary above the jet and the test with one horizontal boundary below differ from the theoretical results by approximately the same amount but in opposite directions, making the average virtually correct. The average is considered to represent Case V.

Free air conditions were assumed to be represented by the average corrected results of Cases I,II,IV, and V.

The experimental correction factors were calculafed from the equations:

$$\delta_D = \frac{\Delta C_D}{\frac{S}{C} C_L^2}$$

$$\delta_\alpha = \frac{\Delta\alpha}{\frac{S}{C} c_L \frac{180}{\pi}}$$

where δ_D = correction factor for drag.

δ_α = correction factor for angle of attack.

ΔC_D = difference between free air drag and actual test drag at the same lift coefficient.

$\Delta\alpha$ = difference between free air angle of attack and actual test angle of attack at the same lift coefficient.

Theoretical and experimental drag and angle of attack corrections are presented in Figures 14 to 25. From these the experimental correction factors for drag and angle of attack were computed for several lift coefficients and listed in Tables IX to XV. The average drag factor and angle of attack factor for each jet type and all lifts were computed and recorded in Tables XVI to XX.

Analysis of Data

When the correction factors for the square jet with several boundary arrangements were applied to the net force test data, the lift - drag polars for Cases IV and V showed large discrepancies. After a review of the test methods showed no apparent possibility of causing errors of such magnitude as were in evidence, the theory was turned to as the probable source of error. A thorough analysis

resulted in discovering that in Case IV an effect of appreciable magnitude had been omitted, and that an arithmetic error had been made in Case V.

In the process of evaluating the series S_4 in Case IV, Ref.3, the line beginning "The entire effect....." should read: The entire effect of all vertical rows of positive doublets extending from $x = mb$ to infinity is thus represented by the effect of a positive vortex row of strength $\frac{\Gamma\Delta L}{b}$ located at $x = (p + 1/2)b$, where p is the number of the last doublet taken into account, and a negative vortex row of the same strength at x = infinity. Then in Table I of Ref. 3 :

$$\delta_4 = \frac{\pi}{4}r\left(\sum_{1}^{p}\frac{1}{\sinh^2 m\pi r} - \frac{1}{6}\right) + \frac{1}{4}\coth\left(p + \frac{1}{2}\right)\pi r$$

should be

$$\delta_4 = \frac{\pi}{4}r\left(\sum_{1}^{p}\frac{1}{\sinh^2 m\pi r} - \frac{1}{6}\right) + \frac{1}{4}\coth\left(p + \frac{1}{2}\right)\pi r - \frac{1}{4}\coth$$

$$= \frac{\pi}{4}r\left(\sum_{1}^{p}\frac{1}{\sinh^2 m\pi r} - \frac{1}{6}\right) + \frac{1}{4}\coth\left(p + \frac{1}{2}\right)\pi r - 0.250$$

Correct values of δ_4 obtained by subtracting 0.250 are tabulated in Table XXI.

In Case V there is an arithmetic error in transferring from

$$v_T = \frac{\Gamma\Delta L}{2\pi}\left(\frac{\pi}{2h}\right)^2\left[\frac{1}{12} + S_3'\right]$$

to

$$\delta_5 = \frac{\pi}{4}\frac{r}{2}\left(\sum_{1}^{\infty}\frac{(-1)^n\cosh\frac{m\pi r}{2}}{\sinh^2\frac{m\pi r}{2}} + \frac{1}{12}\right)$$

This should be

$$\delta_5 = \frac{\pi}{16} r \left(\sum_{1}^{\infty} \frac{(-1)^n \cosh^2 \frac{m\pi r}{2}}{\sinh^2 \frac{m\pi r}{2}} + \frac{1}{12} \right)$$

The corrected factors, which are one half the magnitude of those in Table I, Ref.3, are in Table XXI of this report.

Referring to Figures 11 to 13 we see that drag and angle of attack corrected for jet boundary effect are equal to free air drag and angle of attack $\pm$ 2 percent maximum, except in Case III which is as much as 3 percent too high. It has been mentioned earlier in this report that Case III does not show close agreement between theory and experiment. Theory gives δ = 0.000 but experiment gives δ_D = -0.021 and δ_α = - 0.069 (Table XVIII).

It is interesting to note the similarity in the shape of $C_L - \Delta C_D$ and $C_L - \Delta\alpha$ curves for all cases (Figures 14 to 25).

Tables IX to XV show the experimental correction factors for several lift coefficients as well as the average for all lifts.

Average results of the experimental tests are compared with theory in Tables XVI to XX. Excellent agreement was found to exist between theory and experiment for the closed tunnel except in the experimentally determined drag correction for the 3" x 18" airfoil. This discrepancy cannot be accounted for at present. Likewise, good agreement was found for the open jet except in the experimental angle of attack correction. The jets with vertical boundaries and with one horizontal boundary show

satisfactory agreement.

Theoretical corrections are listed in Table XXI and are plotted against the jet width to height ratio b/h in Fig. 1. The incorrect curves as calculated in Ref. 3 are indicated by broken lines.

Conclusions

On the basis of these tests the following conclusions are made:

1. Theodorsen's method of arranging image systems in determining theoretical jet boundary corrections for square tunnels is satisfactory for ratios of span to tunnel width up to 60 percent, the maximum observed in these tests.

2. The tests showed that Theodorsen's corrections for Cases IV and V were incorrect. The values determined as a result of this investigation are $\delta_4 = -.126$ and $\delta_5 = -.063$.

3. After application of the boundary interference factors, corrected in Cases IV and V, the lift versus the drag and lift versus angle of attack curves are equivalent to free air conditions within $\pm$ 2 percent, except in Case III which is 3 percent too large.

4. Theory gives $\delta = .000$ but experiment gives $\delta_D = -.021$ and $\delta_\alpha = -.069$, for Case III.

5. A single jet boundary above an airfoil does not produce the same interference as a boundary below. The average experimental effect of the two conditions agrees with theory.

6. The arrangement of " slots and slats" of equal width around the square jet did not give zero correction.

It is believed that a greater slat to slot ratio will produce equivalent free air conditions.

Acknowledgements

It is with pleasure that I acknowledge the assistance of Professor Montgomery Knight who suggested the investigation and made helpful comments and criticisms, Professor W. B. Johns to whom thanks are due for his analysis of the corrections of Theodorsen's theory in Cases IV and V, and Mr. W. C. Slocum who helped in the construction of the boundary walls.

Daniel Guggenheim School of Aeronautics,
Georgia School of Technology,
Atlanta, Georgia., May 11, 1934.

REFERENCES AND BIBLIOGRAPHY

1. Prandtl, L.: Application of Modern Hydrodynamics to Aeronautics. T.R. No.116, N.A.C.A., 1921.

2. Glauert, H.: The Elements of Aerofoil and Airscrew Theory. Chap.XIV. Cambridge University Press, 1930.

3. Theodorsen, Theodore : The Theory of Wind-Tunnel Wall Interference. T.R. No.410, N.A.C.A. Annual Report, 1932.

4. Theodorsen, Theodore : Interference on an Airfoil of Finite Span in an Open Rectangular Wind Tunnel. T.R. No.461, N.A.C.A., 1933.

5. Smithsonian Physical Tables. 1923 Edition. Page 125.

6. Knight, Montgomery, and Thomas A. Harris: Experimental Determination of Jet Boundary Corrections for Airfoil Tests in Four Open Wind Tunnel Jets of Different Shapes. T.R. No.361, N.A.C.A., 1930.

7. Higgins, George J.: Wall Interference in Closed Type Wind Tunnels. T.R. No.256, N.A.C.A., 1927.

8. Higgins, George J.: The Effect of Walls in Closed Type Wind Tunnels. T.R. No.275, N.A.C.A., 1927.

9. Rosenhead, L.: Interference Due to Walls of a Wind Tunnel. Royal Society Proceedings, Oct.-Nov., 1933, pp. 308-320.

TABLE I - FORCE TEST

Case I - closed tunnel

Clark Y airfoil 3"x 18"

C_L	C_D'	$*\Delta C_D$	C_D	α'	$*\Delta\alpha$	α
0	.0239	.0000	.0239	0	0	0
0.094	.0219	.0001	.0220	1.05	.04	1.09
.188	.0212	.0003	.0215	2.10	.09	2.19
.375	.0235	.0012	.0247	4.25	.17	4.42
.563	.0316	.0026	.0342	6.45	.26	6.71
.751	.0441	.0046	.0487	8.75	.35	9.10
.938	.0604	.0072	.0676	11.15	.44	11.59
1.127	.0817	.0104	.0921	13.75	.53	14.28
1.221	.0956	.0121	.1077	15.25	.57	15.82

* Theoretical corrections.

TABLE II - FORCE TEST

Case I - closed tunnel

Clark Y airfoil 3" x12"

C_L	C_D'	$*\Delta C_D$	C_D	α'	$*\Delta\alpha$	α
0	.0259	.0000	.0259	0	0	0
.141	.0244	.0001	.0245	1.95	.04	1.99
.282	.0265	.0004	.0269	3.85	.09	3.94
.422	.0329	.0010	.0339	5.80	.13	5.93
.563	.0438	.0017	.0455	7.80	.18	7.98
.704	.0579	.0027	.0606	9.85	.22	10.07
.845	.0752	.0039	.0791	11.95	.26	12.21
.986	.0959	.0053	.1012	14.10	.31	14.41
1.127	.1218	.0069	.1287	16.35	.35	16.70

* Theoretical corrections.

TABLE III - FORCE TEST

Case II - Free jet

Clark Y airfoil 3"x18"

C_L	C'_D	$^*\Delta C_D$	C_D	α'	$^*\Delta\alpha$	α
0	.0239	.0000	.0239	0	0	0
0.094	.0220	-.0001	.0219	1.15	-.04	1.11
.188	.0217	-.0003	.0214	2.25	-.09	2.16
.375	.0257	-.0011	.0246	4.55	-.17	4.38
..563	.0356	-.0026	.0330	6.95	-.26	6.69
.751	.0512	-.0046	.0466	9.40	-.35	9.05
.938	.0733	-.0072	.0661	12.00	-.44	11.56
1.127	.1016	-.0103	.0913	14.75	-.53	14.22
1.221	.1185	-.0121	.1064	16.25	-.57	15.68

* Theoretical corrections.

TABLE IV - FORCE TEST

Case II - Free jet

Clark Y airfoil 3"x 12"

C_L	C'_D	$^*\Delta C_D$	C_D	α'	$^*\Delta\alpha$	α
0	.0259	.0000	.0259	0	0	0
.141	.0248	-.0001	.0247	2.00	-.04	1.96
.282	.0277	-.0004	.0273	4.05	-.09	3.96
.422	.0354	-.0010	.0344	6.10	-.13	5.97
.563	.0468	-.0017	.0451	8.20	-.18	8.02
.704	.0625	-.0027	.0598	10.30	-.22	10.08
.845	.0827	-.0039	.0788	12.45	-.26	12.19
.986	.1069	-.0053	.1016	14.65	-.31	14.34
1.127	.1356	-.0069	.1287	17.00	-.35	16.65

* Theoretical corrections.

TABLE V - FORCE TEST

Case III - Horizontal boundaries

Clark Y airfoil 3"x18"

C_L	C_D'	$^*\Delta C_D$	C_D	α'	$^*\Delta\alpha$	α
0	.0239	.000	.0239	0	.00	0
.094	.0223	.000	.0223	1.10	.00	1.10
.188	.0219	.000	.0219	2.20	.00	2.20
.375	.0253	.000	.0253	4.50	.00	4.50
.563	.0338	.000	.0338	6.85	.00	6.85
.751	.0481	.000	.0481	9.25	.00	9.25
.938	.0681	.000	.0681	11.85	.00	11.85
1.127	.0938	.000	.0938	14.65	.00	14.65
1.221	.1097	.000	.1097	16.15	.00	16.15

* Theoretical corrections.

TABLE VI - FORCE TEST

Case IV - Vertical boundaries

Clark Y airfoil 3"x18"

C_L	C_D'	$^*\Delta C_D$	C_D	α'	$^*\Delta\alpha$	α
0	.0239	.0000	.0239	0	0	0
.094	.0222	-.0001	.0221	1.15	-.04	1.11
.188	.0225	-.0003	.0222	2.30	-.08	2.22
.375	.0266	-.0010	.0256	4.60	-.16	4.44
.563	.0359	-.0023	.0336	7.00	-.24	6.76
.751	.0513	-.0042	.0471	9.45	-.32	9.13
.938	.0727	-.0065	.0662	12.05	-.40	11.65
1.127	.0997	-.0094	.0903	14.90	-.48	14.42
1.221	.1152	-.0109	.1043	16.45	-.52	15.93

* Theoretical corrections.

TABLE VII - FORCE TEST

Case V - One horizontal boundary

Clark Y airfoil 3" x 18"

C_L	C'_D	$^*\Delta C_D$	C_D	α'	$^*\Delta\alpha$	α
0	.0239	.0000	.0239	0	0	0
.094	.0221	.0000	.0221	1.15	-.02	1.13
.188	.0218	-.0001	.0217	2.25	-.04	2.21
.375	.0251	-.0005	.0246	4.60	-.08	4.52
.563	.0341	-.0012	.0329	6.90	-.12	6.78
.751	.0483	-.0021	.0462	9.35	-.16	9.19
.938	.0682	-.0033	.0649	11.85	-.20	11.65
1.127	.0942	-.0048	.0894	14.60	-.24	14.36
1.221	.1101	-.0056	.1045	16.15	-.26	15.89

* Theoretical corrections.

TABLE VIII - THEORETICAL δ

(Table I in Ref.3)

r	δ_1	δ_2	δ_3	δ_4	δ_5
0	∞	$-\infty$	$-\infty$	∞	$-\infty$
.125	1.055	-0.524	-0.524	1.051	-1.050
.25	.523	- .262	- .262	.524	- .524
.50	.263	- .137	- .127	.262	- .262
.625	.213	- .122	- .089	.210	- .208
.75	.175	- .120	- .056	.161	- .173
1.00	.138	- .137	.000	.124	- .127
1.50	.120	- .197	.077	.054	- .056
2.00	.137	- .262	.126	- .012	.000
4.00	.262	- .524	.262	- .276	.126
∞	∞	$-\infty$	∞	$-\infty$	∞

TABLE IX - EXPERIMENTAL δ
Case I - closed tunnel
Clark Y airfoil 3" x 18"

$$\delta_D = \frac{\Delta C_D}{\frac{S}{C} C_L^2} \qquad \delta_\alpha = \frac{\Delta \alpha}{\frac{S}{C} C_L \frac{180}{\pi}}$$

C_L	C_D	δ_D	α	δ_α
0.1	(.0002)	(.336)	.05	.146
.2	(.0007)	(.293)	.09	.132
.3	(.0013)	(.243)	.14	.137
.4	.0016	.168	.20	.146
.5	.0019	.128	.26	.152
.6	.0023	.109	.30	.146
.7	.0031	.106	.34	.142
.8	.0043	.113	.38	.139
.9	.0058	.121	.43	.140
1.0	.0075	.126	.49	.143
1.1	.0093	.129	.54	.144
1.2	.0108	.126	.56	.137
Average		.125		.142

Quantities in () not averaged because of large discrepancies.
C_D from Fig.14. α from Fig.21

TABLE X - EXPERIMENTAL δ
Case I - closed tunnel
Clark Y airfoil 3" x 12"

$$\delta_D = \frac{\Delta C_D}{\frac{S}{C} C_L^2} \qquad \delta_\alpha = \frac{\Delta \alpha}{\frac{S}{C} C_L \frac{180}{\pi}}$$

C_L	C_D	δ_D	α	δ_α
0.1	(.0001)	(.252)	(.02)	(.088)
.2	(.0003)	(.189)	.06	.132
.3	.0006	.168	.11	.161
.4	.0011	.174	.14	.154
.5	.0014	.142	.18	.158
.6	.0016	.113	.21	.154
.7	.0022	.114	.23	.144
.8	.0032	.126	.24	.132
.9	.0044	.137	.26	.127
1.0	.0057	.144	.27	.119
1.1	.0066	.138	.31	.120
Average		.140		.140

Quantities in () not averaged because of large discrepancies.
C_D from Fig.15 α from Fig.21

TABLE XI - EXPERIMENTAL δ
Case II - Free jet
Clark Y airfoil 3" x 18"

$$\delta_D = \frac{\Delta C_D}{\frac{S}{C} C_L^2} \qquad \delta_\alpha = \frac{\Delta \alpha}{\frac{S}{C} C_L \frac{180}{\pi}}$$

C_L	C_D	δ_D	α	δ_α
0.1	(.0003)	(.503)	(.05)	(.142)
.2	.0004	.168	(.07)	(.103)
.3	.0007	.131	(.10)	(.097)
.4	.0012	.126	(.13)	(.095)
.5	.0019	.128	(.18)	(.106)
.6	.0026	.121	.23	.112
.7	.0033	.113	.27	.113
.8	.0044	.116	.32	.117
.9	.0060	.125	.38	.124
1.0	.0082	.138	.43	.126
1.1	.0101	.140	.45	.120
1.2	.0117	.137	.45	.110
Average		-.132		-.117

Quantities in () not averaged because of large discrepancies.
C_D from Fig.16. α from Fig.22

TABLE XII - EXPERIMENTAL δ
Case II - Free jet
Clark Y airfoil 3" x 12"

$$\delta_D = \frac{\Delta C_D}{\frac{S}{C} C_L^2} \qquad \delta_\alpha = \frac{\Delta \alpha}{\frac{S}{C} C_L \frac{180}{\pi}}$$

C_L	C_D	δ_D	α	δ_α
0.1	(.0001)	(.252)	(.04)	(.176)
.2	(.0003)	(.189)	.07	.154
.3	(.0007)	(.197)	.08	.117
.4	(.0012)	(.190)	.14	.154
.5	.0014	.142	(.19)	(.167)
.6	.0016	.113	.20	.146
.7	.0023	.119	.22	.138
.8	.0033	.130	.24	.132
.9	.0045	.141	.26	.127
1.0	.0057	.144	.28	.123
1.1	.0066	.138	.31	.124
Average		-.131		-.137

Quantities in () not averaged because of large discrepancies.
C_D from Fig.17. α from Fig.22

TABLE XIII - EXPERIMENTAL δ
Case III - Horizontal boundaries
Clark Y airfoil 3" x 18"

$$\delta_D = \frac{\Delta C_D}{\frac{S}{C} C_L^2} \qquad \delta_\alpha = \frac{\Delta \alpha}{\frac{S}{C} C_L \frac{180}{\pi}}$$

C_L	C_D	δ_D	α	δ_α
0.1	(.0002)	(.336)	(.00)	(.000)
.2	(.0001)	(.084)	(.02)	(.029)
.3	.0001	.019	.05	.043
.4	.0002	.042	.08	.059
.5	.0002	.013	.10	.073
.6	.0001	.005	.11	.054
.7	.0002	.007	.13	.054
.8	.0005	.013	.16	.059
.9	.0010	.021	.22	.072
1.0	.0015	.025	.30	.088
1.1	.0021	.029	.35	.093
1.2	.0028	.033	.34	.083
Average		-.021		-.069

Quantities in () not averaged because of large discrepancies.
C_D from Fig.18. α from Fig.23.

TABLE XIV - EXPERIMENTAL δ
Case IV - Vertical boundaries
Clark Y airfoil 3" x 18"

$$\delta_D = \frac{\Delta C_D}{\frac{S}{C} C_L^2} \qquad \delta_\alpha = \frac{\Delta \alpha}{\frac{S}{C} C_L \frac{180}{\pi}}$$

C_L	C_D	δ_D	α	δ_α
0.1	(.0001)	(.168)	(.05)	(.147)
.2	(.0007)	(.293)	(.12)	(.176)
.3	(.0013)	(.224)	.14	.137
.4	(.0016)	(.168)	.18	.132
.5	.0020	.134	.23	.135
.6	.0024	.112	.28	.137
.7	.0030	.103	.32	.134
.8	.0041	.108	.36	.132
.9	.0054	.112	.42	.137
1.0	.0067	.113	.50	.147
1.1	.0086	.111	.58	.155
1.2	(.0085)	(.099)	.61	.149
Average		-.113		-.139

Quantities in () not averaged because of large discrepancies.
C_D from Fig.19. α from Fig.24.

TABLE XV - EXPERIMENTAL δ
Case V - One horizontal boundary
Clark Y airfoil 3" x 18"

$$\delta_D = \frac{\Delta C_D}{\frac{S}{C} C_L^2} \qquad \delta_\alpha = \frac{\Delta \alpha}{\frac{S}{C} C_L \frac{180}{\pi}}$$

C_L	C_D	δ_D	α	δ_α
0.1	(.0002)	(.336)	(.04)	(.117)
.2	(.0003)	(.126)	(.06)	(.088)
.3	.0005	.093	(.05)	(.049)
.4	.0009	.095	(.04)	(.029)
.5	.0012	.081	(.07)	(.041)
.6	.0016	.075	.09	.044
.7	.0021	.075	.11	.046
.8	.0026	.068	.15	.055
.9	.0030	.062	.18	.059
1.0	.0033	.055	.23	.067
1.1	.0038	.053	.27	.072
1.2	.0048	.056	.28	.068
Average		-.071		-.059

Quantities in () not averaged because of large discrepancies.
C_D from Fig.20 α from Fig.25.

TABLE XVI - CORRECTION FACTORS
Square closed tunnel

	3" x 12" airfoil		3" x 18" airfoil	
	δ_D	δ_α	δ_D	δ_α
Theoretical	.138	.138	.138	.138
Experimental	.140	.140	.125	.142

TABLE XVII - CORRECTION FACTORS
Square open jet

	3" x 12" airfoil		3" x 18" airfoil	
	δ_D	δ_α	δ_D	δ_α
Theoretical	-.137	-.137	-.137	-.137
Experimental	-.131	-.137	-.132	-.117

TABLE XVIII- CORRECTION FACTORS
Square jet with horizontal boundaries

3" x 18" airfoil

	δ_D	δ_α
Theoretical	.000	.000
Experimental	- .021	- .069

TABLE XIX - CORRECTION FACTORS
Square jet with vertical boundaries

3" x 18" airfoil

	δ_D	δ_α
Theoretical	- .126	- .126
Experimental	- .113	- .139

TABLE XX - CORRECTION FACTORS
Square jet with one horizontal boundary

3" x 18" airfoil

	δ_D	δ_α
Theoretical	- .063	-.063
Experimental	- .071	-.059

TABLE XXI - THEORETICAL δ
(With δ_4 and δ_5 of Table I, Ref.3, Corrected)

r	δ_1	δ_2	δ_3	δ_4	δ_5
0	∞	$-\infty$	$-\infty$	∞	$-\infty$
.125	1.055	-0.524	-0.524	0.801	-0.525
.250	.523	- .262	- .262	.274	- .262
.50	.263	- .137	- .127	.012	- .131
.625	.213	- .122	- .089	- .040	- .104
.75	.175	- .120	- .056	- .089	- .086
1.00	.138	- .137	.000	- .126	- .063
1.50	.120	- .197	.077	- .196	- .028
2.00	.137	- .262	.126	- .262	.000
4.00	.262	- .524	.262	- .526	.063
∞	∞	$-\infty$	∞	$-\infty$	∞

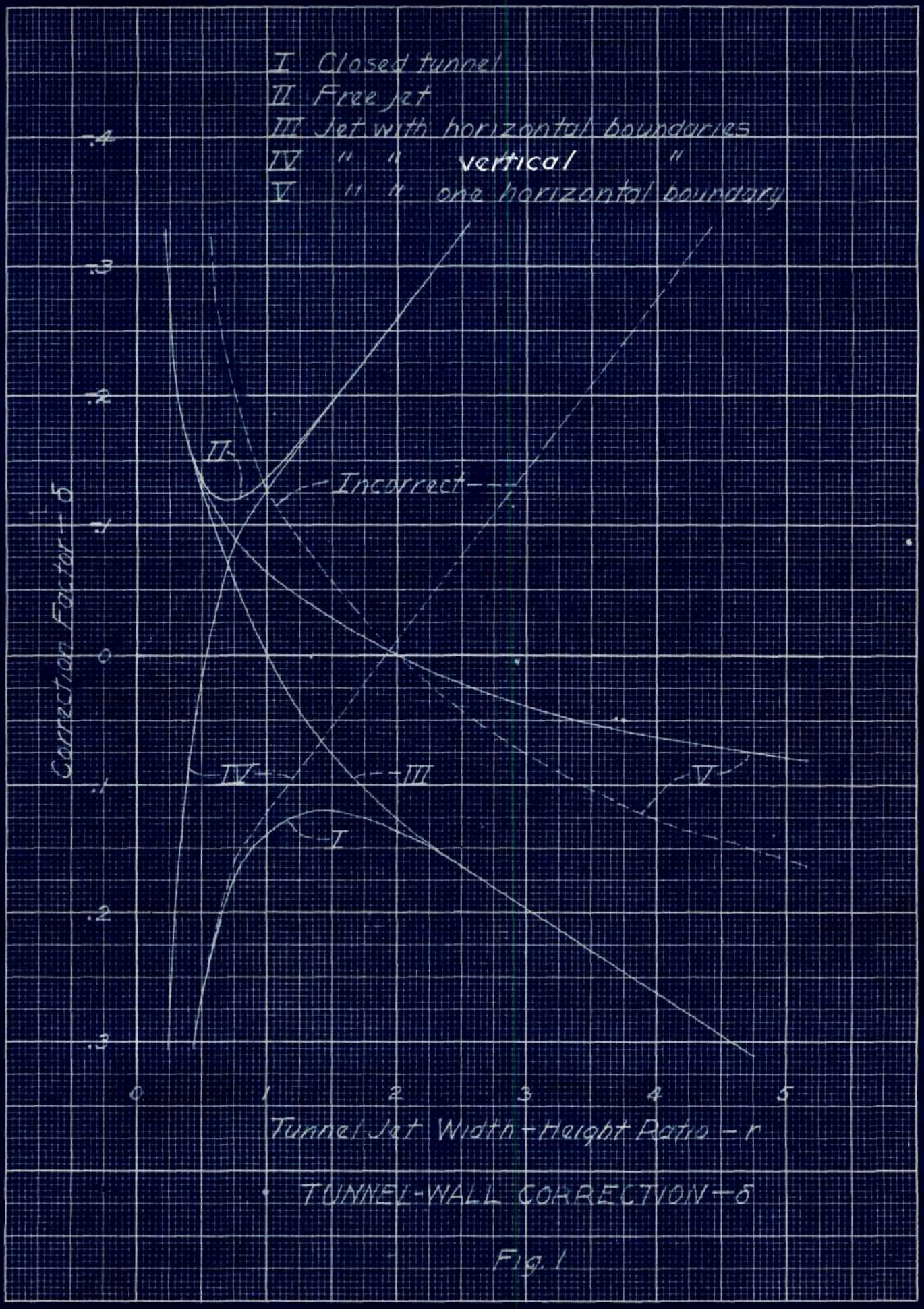

TUNNEL-WALL CORRECTION — δ

Fig. 1

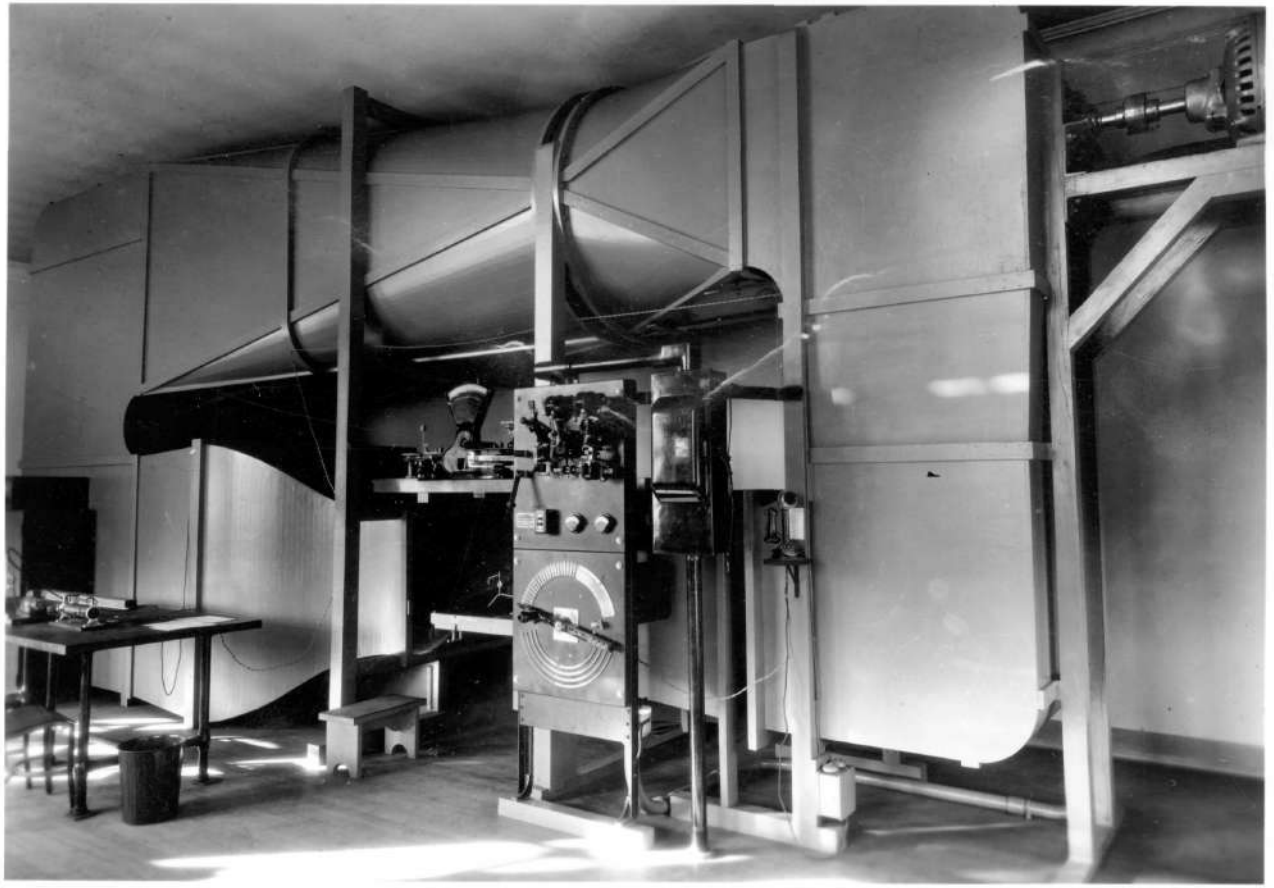

Fig. 2

GEORGIA TECH $2\frac{1}{2}$ FT. OPEN JET WIND TUNNEL

Fig. 3

SIX COMPONENT WIRE BALANCE SYSTEM

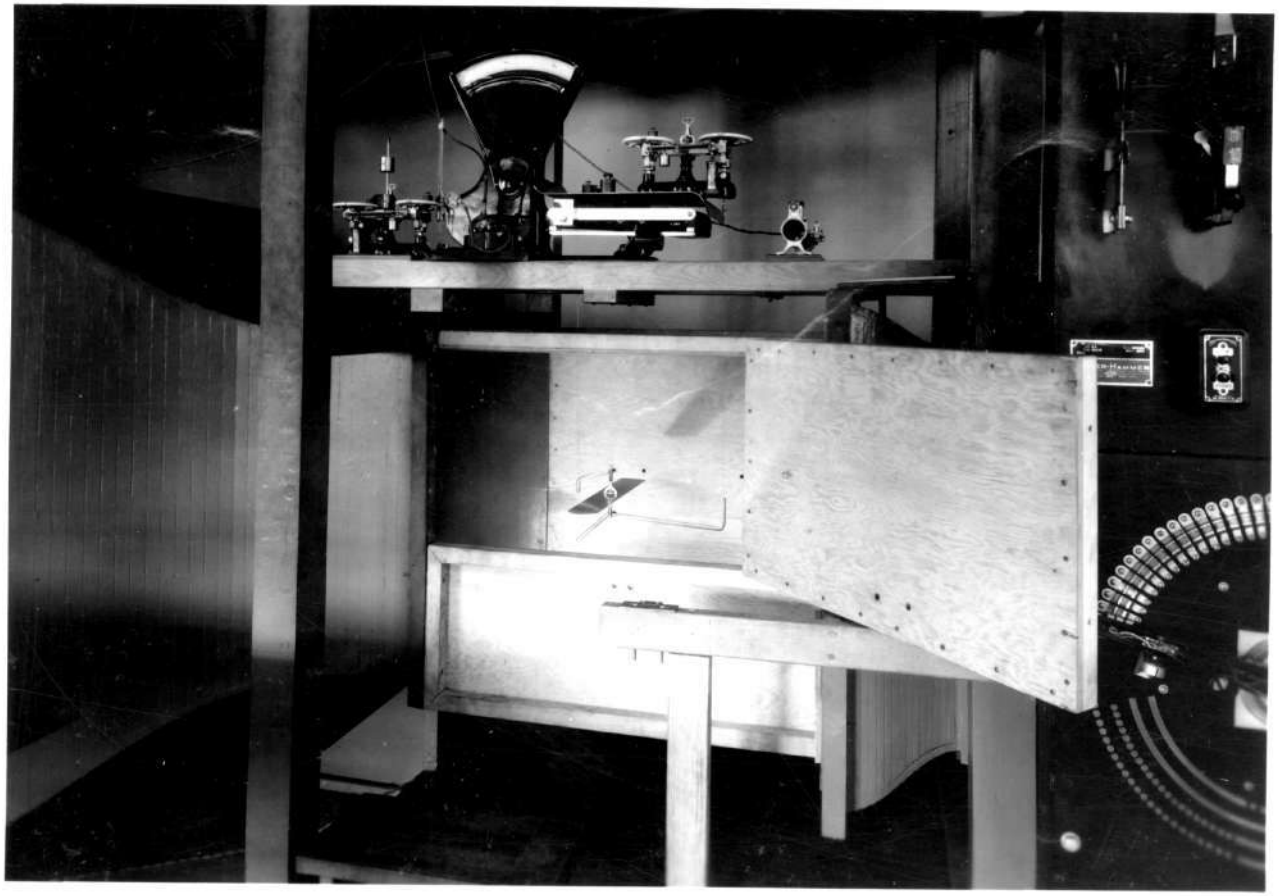

Fig. 4

$2\frac{1}{2}$ FT. CLOSED WIND TUNNEL

Fig: 5

$2\frac{1}{2}$ FT. WIND TUNNEL WITH BOUNDARY OF SLOTS AND SLATS

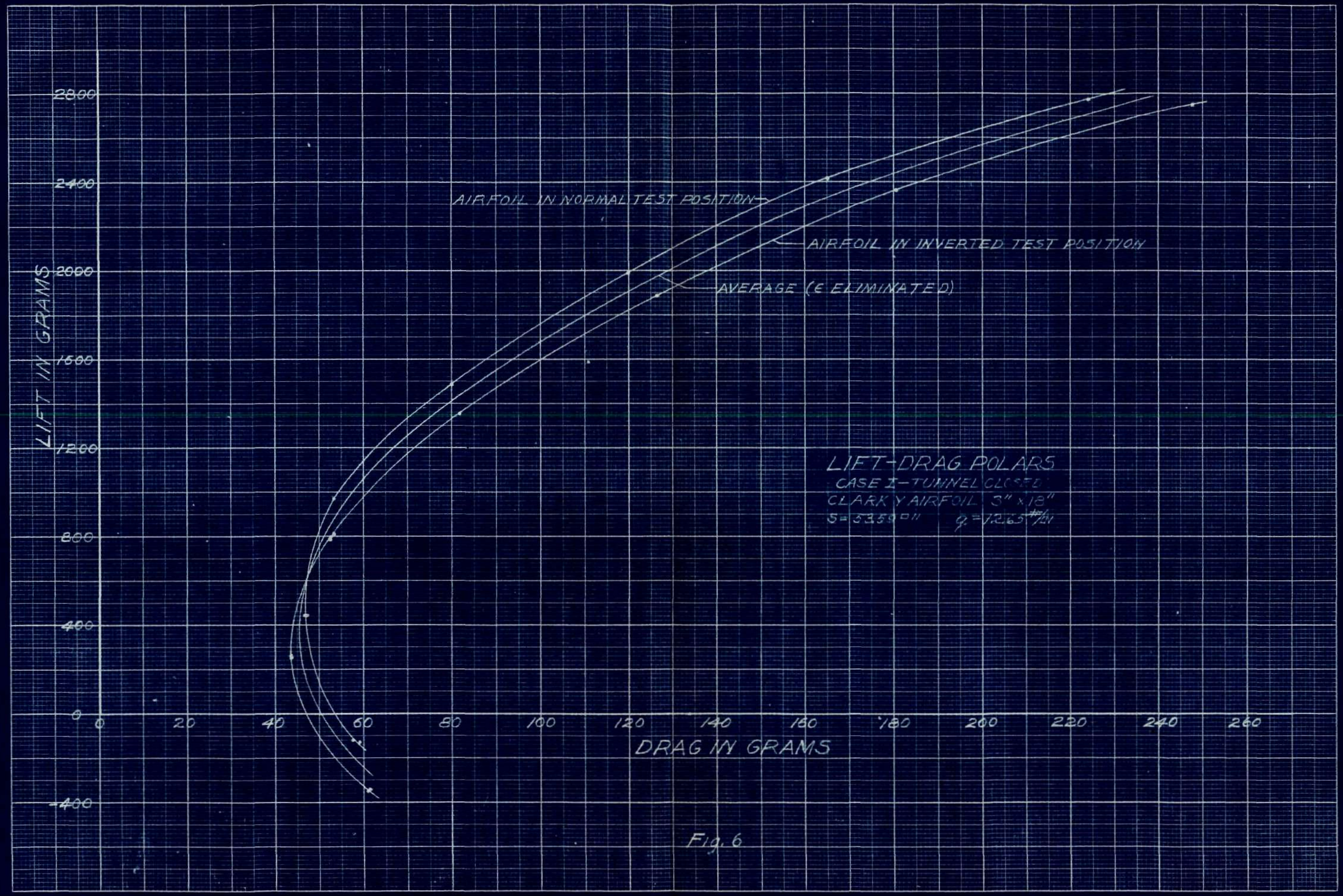
AIRFOIL IN NORMAL TEST POSITION
AIRFOIL IN INVERTED TEST POSITION
AVERAGE (ε ELIMINATED)
LIFT-DRAG POLARS
CASE I—TUNNEL CLOSED
CLARK Y AIRFOIL 3" x 18"
S=3350 □" q=12.65 #/□'
LIFT IN GRAMS
2800
2400
2000
1600
1200
800
400
0
-400
0
20
40
60
80
100
120
140
160
180
200
220
240
260
DRAG IN GRAMS

Fig. 6

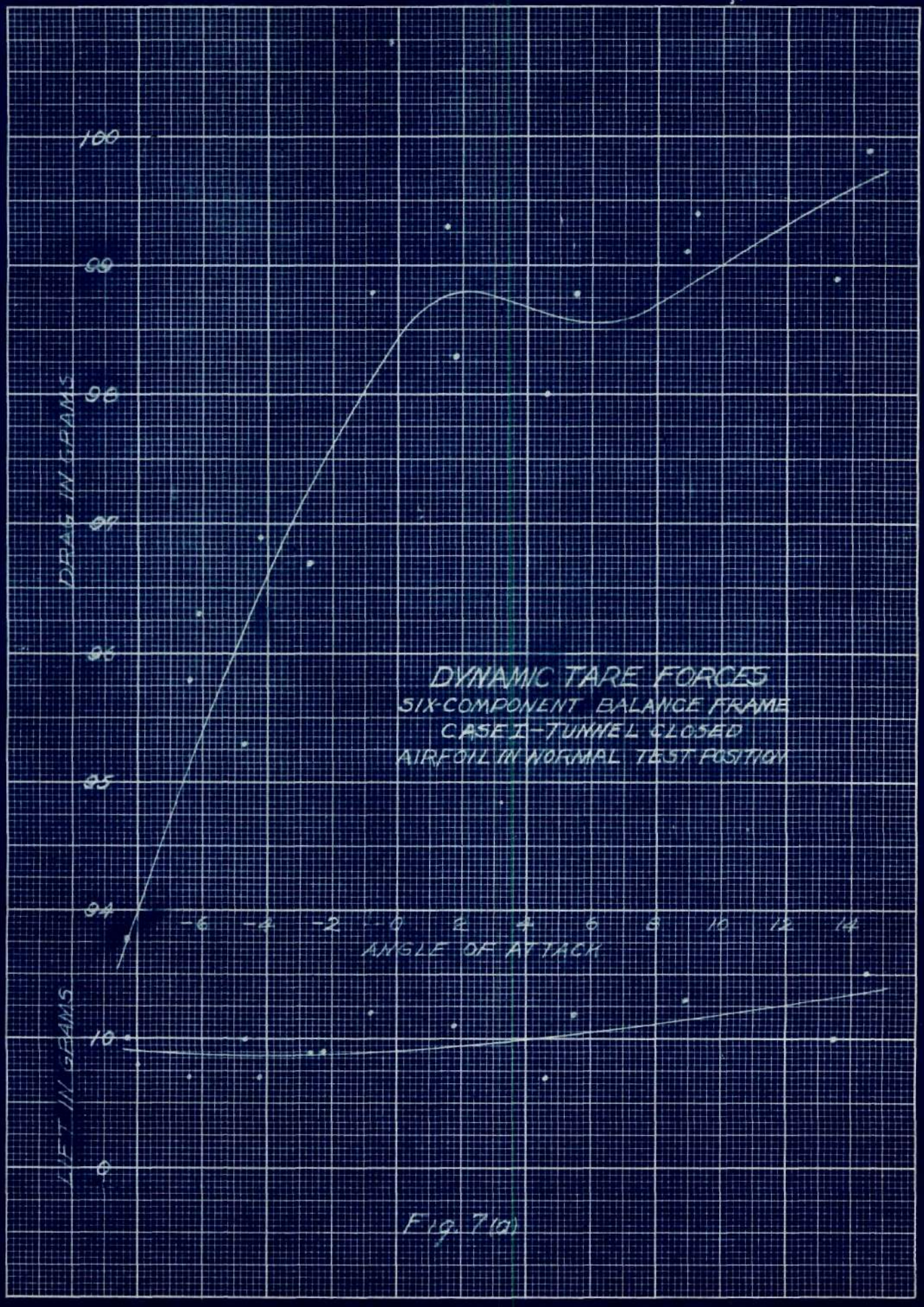

Fig. 7(a)

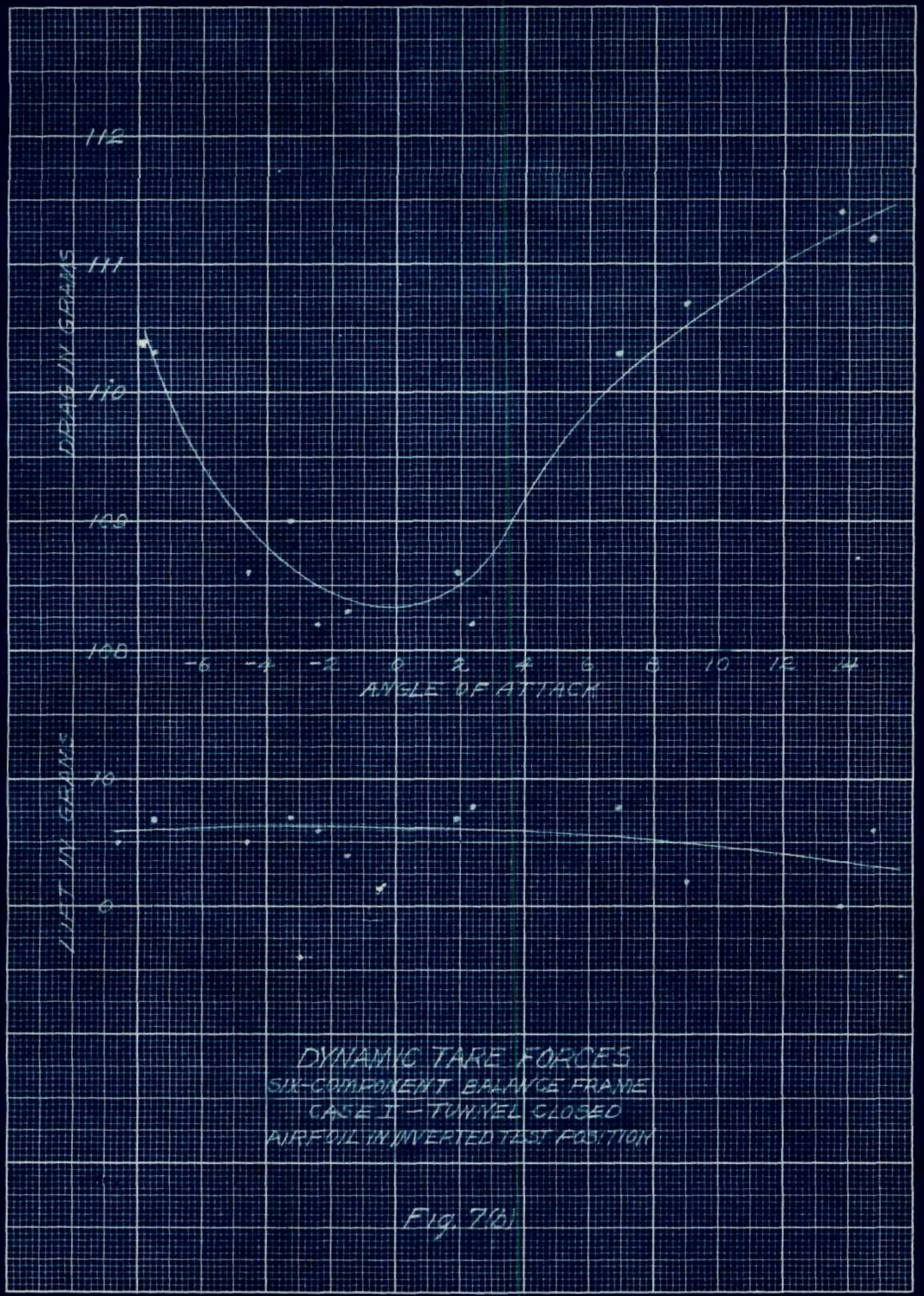

DYNAMIC TARE FORCES
SIX-COMPONENT BALANCE FRAME
CASE I – TUNNEL CLOSED
AIRFOIL IN INVERTED TEST POSITION

Fig. 76)

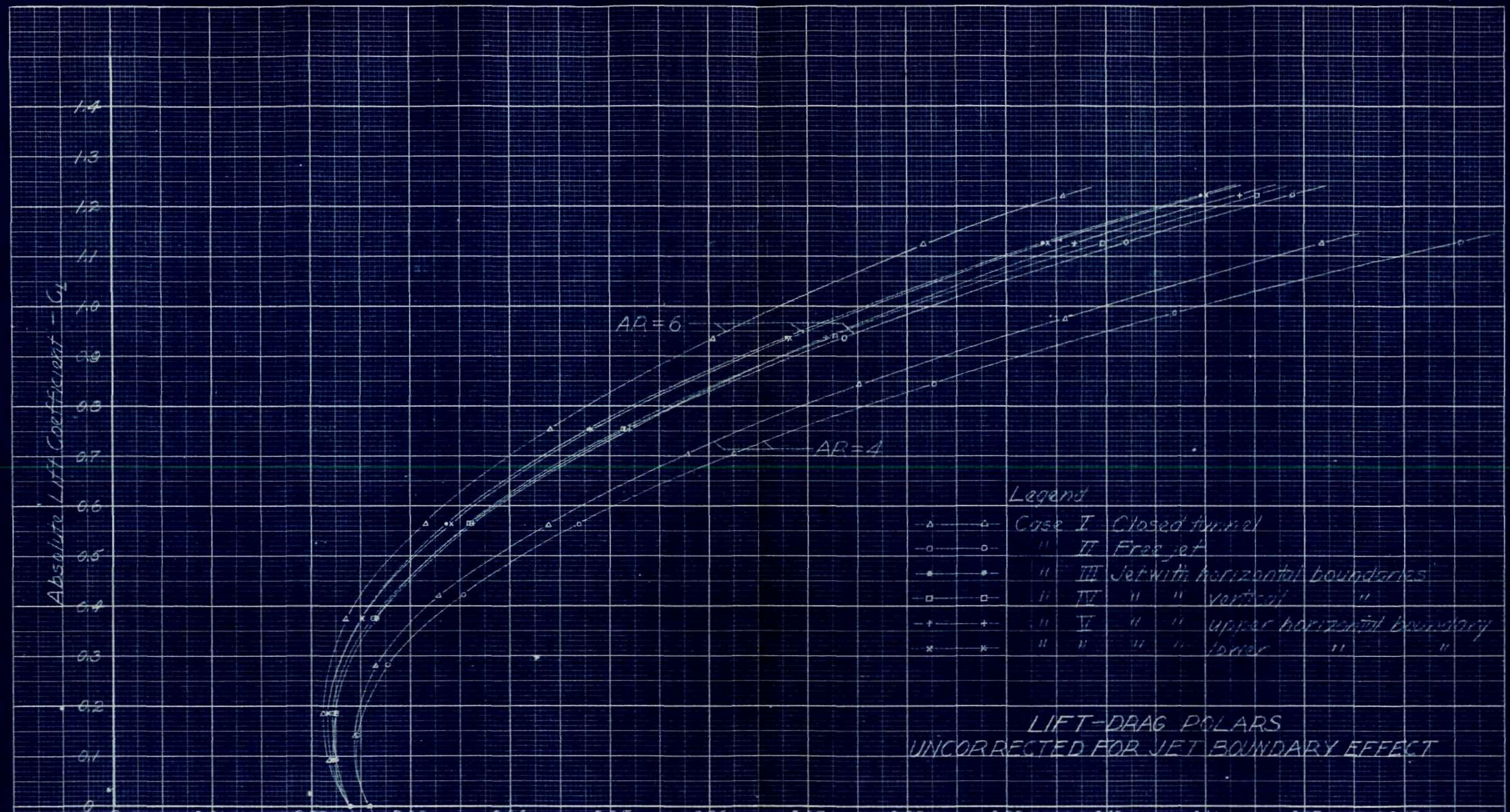
AR=6
AR=4
Legend
Case I Closed tunnel
" II Free jet
" III Jet with horizontal boundaries
" IV " " vertical "
" V " " upper horizontal boundary
" " " " lower " "
LIFT-DRAG POLARS
UNCORRECTED FOR JET BOUNDARY EFFECT
Absolute Lift Coefficient - C_L
Absolute Drag Coefficient - C_D
0
0.1
0.2
0.3
0.4
0.5
0.6
0.7
0.8
0.9
1.0
1.1
1.2
1.3
1.4
0.01
0.02
0.03
0.04
0.05
0.06
0.07
0.08
0.09
0.10
0.11
0.12
0.13

Fig. 8

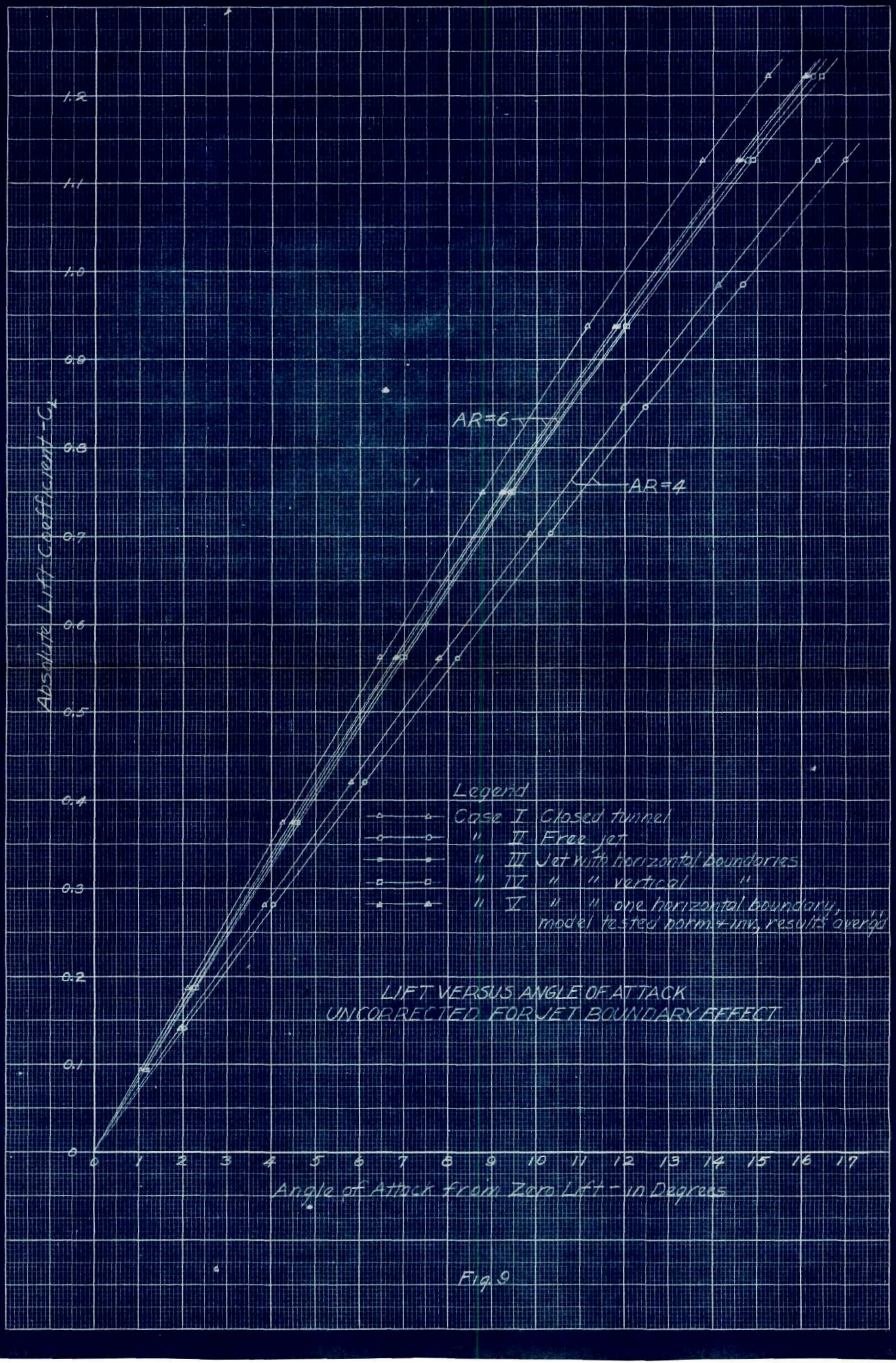
Absolute Lift Coefficient - C_L
1.2
1.1
1.0
0.9
0.8
0.7
0.6
0.5
0.4
0.3
0.2
0.1
0
AR=6
AR=4
Legend
Case I Closed tunnel
" II Free jet
" III Jet with horizontal boundaries
" IV " " vertical "
" V " " one horizontal boundary,
model tested both + and -, results averaged
LIFT VERSUS ANGLE OF ATTACK
UNCORRECTED FOR JET BOUNDARY EFFECT
0 1 2 3 4 5 6 7 8 9 10 11 12 13 14 15 16 17
Angle of Attack from Zero Lift - in Degrees

Fig. 9

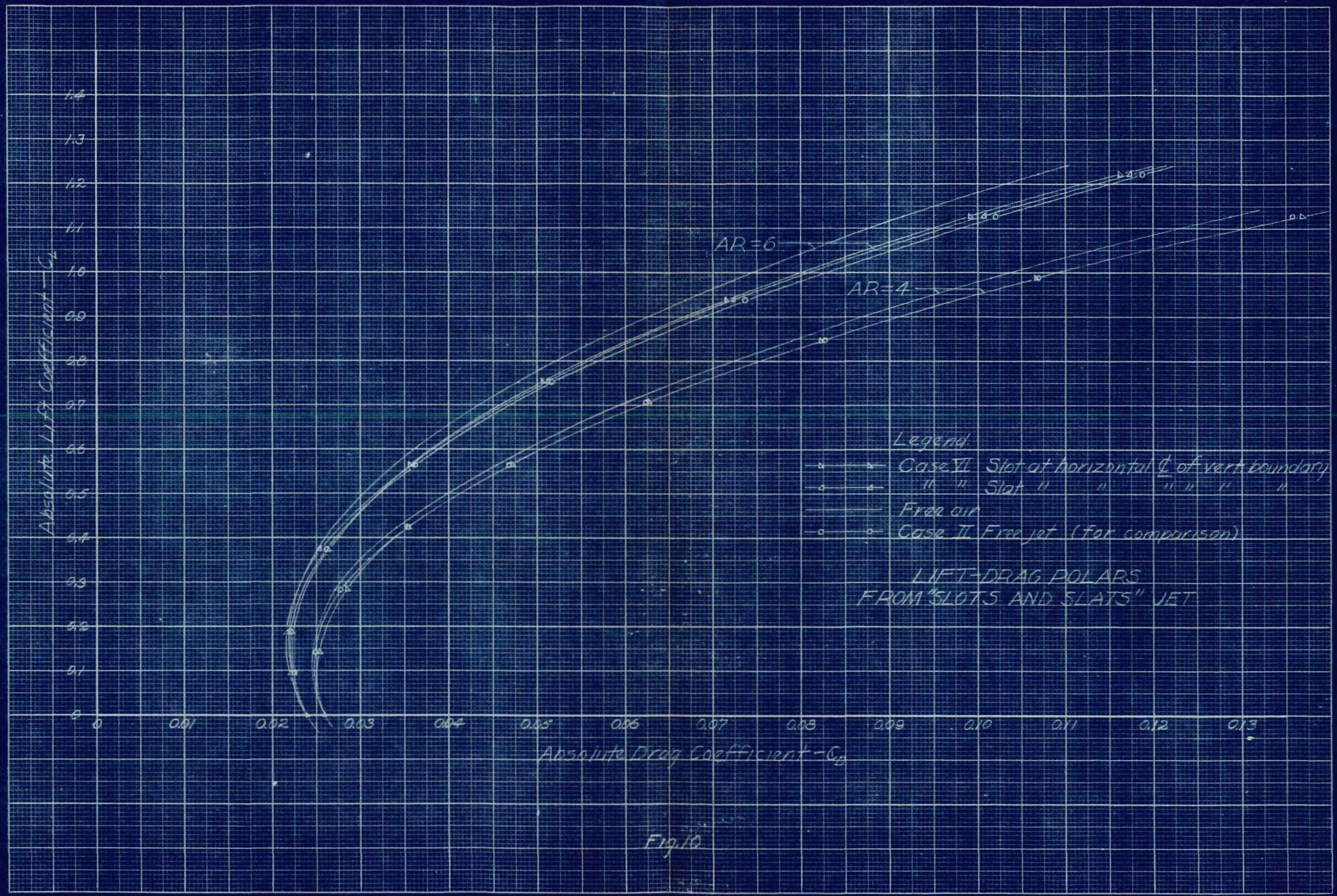
AR=6
AR=4
Legend
Case II Slot at horizontal ℄ of vert boundary
" " Slot " " " " " "
Free air
Case II Free jet (for comparison)
LIFT-DRAG POLARS
FROM "SLOTS AND SLATS" JET
Absolute Lift Coefficient - C_L
Absolute Drag Coefficient - C_D
1.4
1.3
1.2
1.1
1.0
0.9
0.8
0.7
0.6
0.5
0.4
0.3
0.2
0.1
0
0.01
0.02
0.03
0.04
0.05
0.06
0.07
0.08
0.09
0.10
0.11
0.12
0.13

Fig. 10

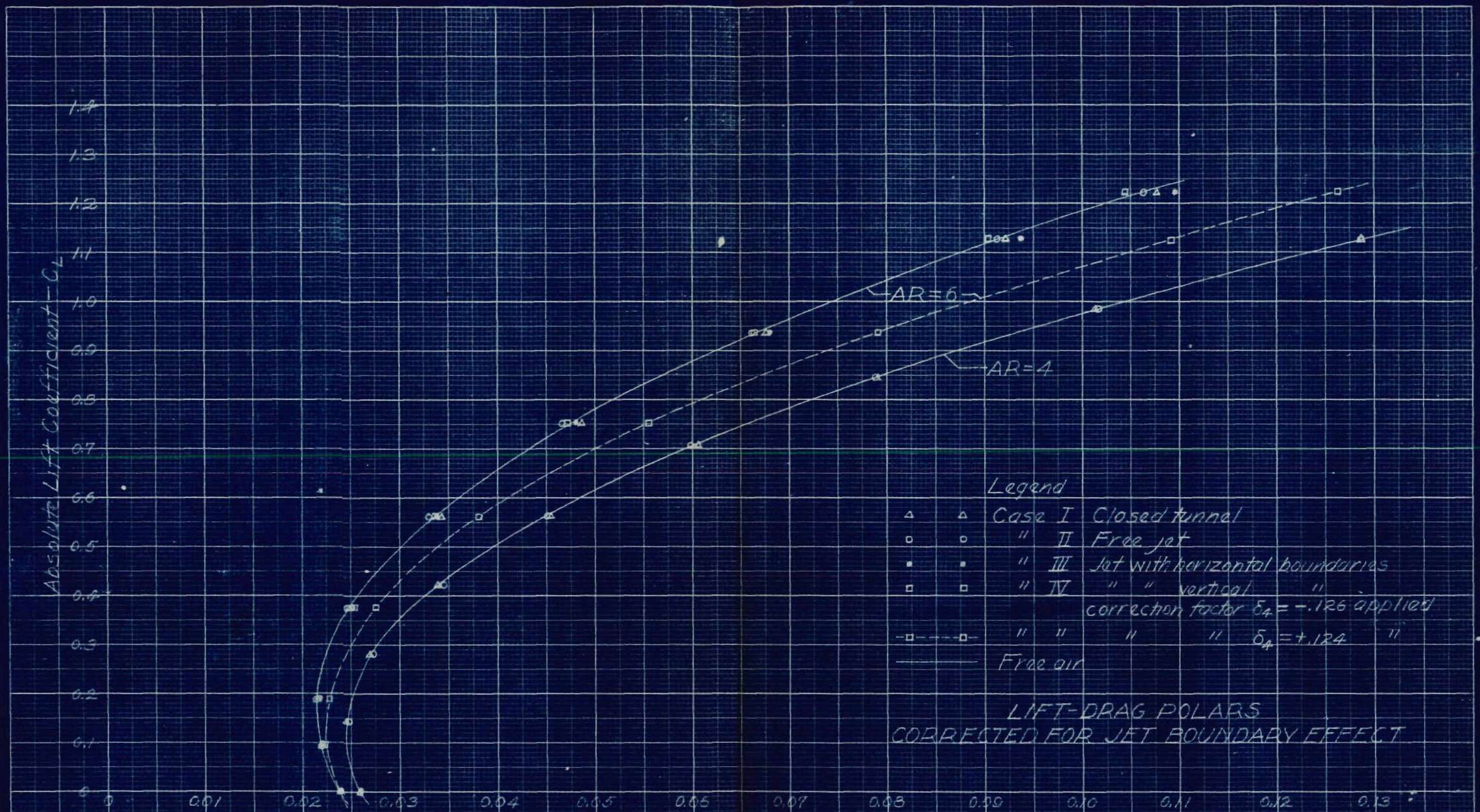
Absolute Lift Coefficient – C_L
1.4
1.3
1.2
1.1
1.0
0.9
0.8
0.7
0.6
0.5
0.4
0.3
0.2
0.1
0
0
0.01
0.02
0.03
0.04
0.05
0.06
0.07
0.08
0.09
0.10
0.11
0.12
0.13
Absolute Drag Coefficient – C_D
AR=6
AR=4
Legend
Case I Closed tunnel
" II Free jet
" III Jet with horizontal boundaries
" IV " " vertical "
correction factor $\delta_4 = -.126$ applied
" " " " $\delta_4 = +.124$ "
Free air
LIFT-DRAG POLARS
CORRECTED FOR JET BOUNDARY EFFECT

Fig. 11

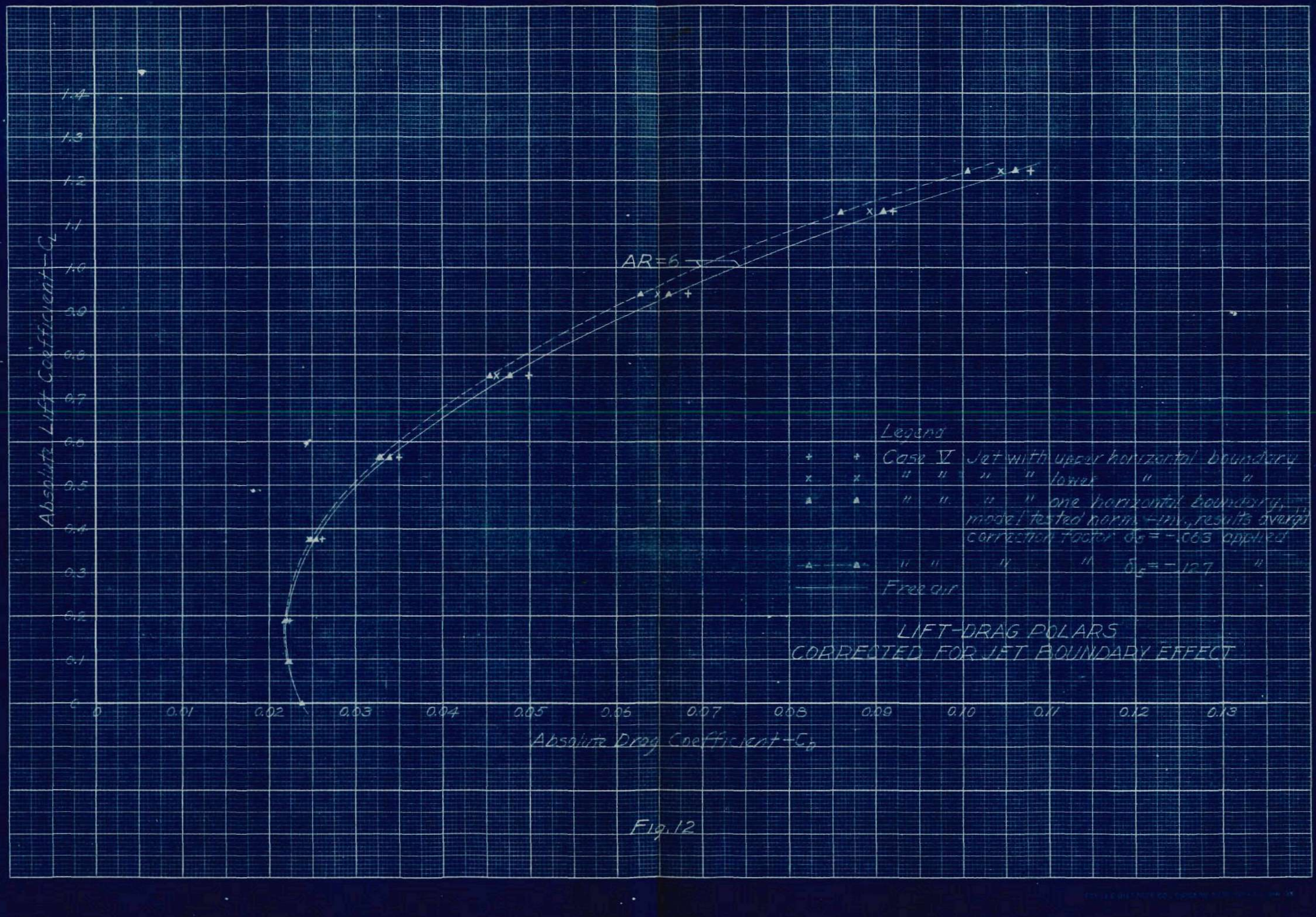
AR=5
Absolute Lift Coefficient - C_L
Absolute Drag Coefficient - C_D
0
0.01
0.02
0.03
0.04
0.05
0.06
0.07
0.08
0.09
0.10
0.11
0.12
0.13
0.1
0.2
0.3
0.4
0.5
0.6
0.7
0.8
0.9
1.0
1.1
1.2
1.3
1.4
Legend
Case V Jet with upper horizontal boundary
" " " " lower " "
" " " " one horizontal boundary, model tested normal to it, results averaged
correction factor $\delta_C = -.063$ applied
" " " " $\delta_C = -.127$ "
Free air
LIFT-DRAG POLARS
CORRECTED FOR JET BOUNDARY EFFECT

Fig. 12

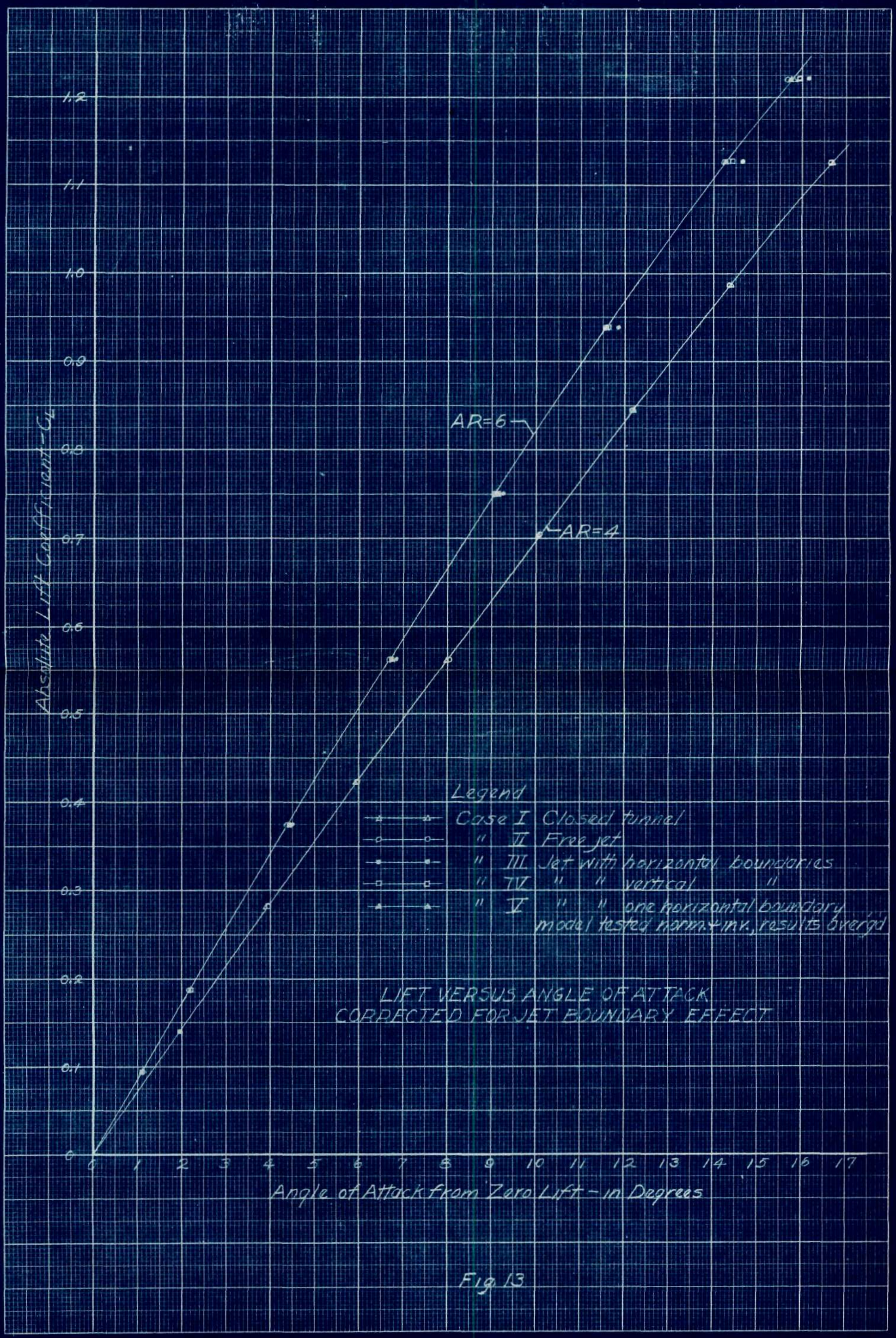
Absolute Lift Coefficient – C_L
1.2
1.1
1.0
0.9
0.8
0.7
0.6
0.5
0.4
0.3
0.2
0.1
0
AR=6
AR=4
Legend
Case I Closed tunnel
" II Free jet
" III Jet with horizontal boundaries
" IV " " vertical "
" V " " one horizontal boundary
model tested norm.+inv., results averaged
LIFT VERSUS ANGLE OF ATTACK
CORRECTED FOR JET BOUNDARY EFFECT
-1 0 1 2 3 4 5 6 7 8 9 10 11 12 13 14 15 16 17
Angle of Attack from Zero Lift – in Degrees

Fig 13

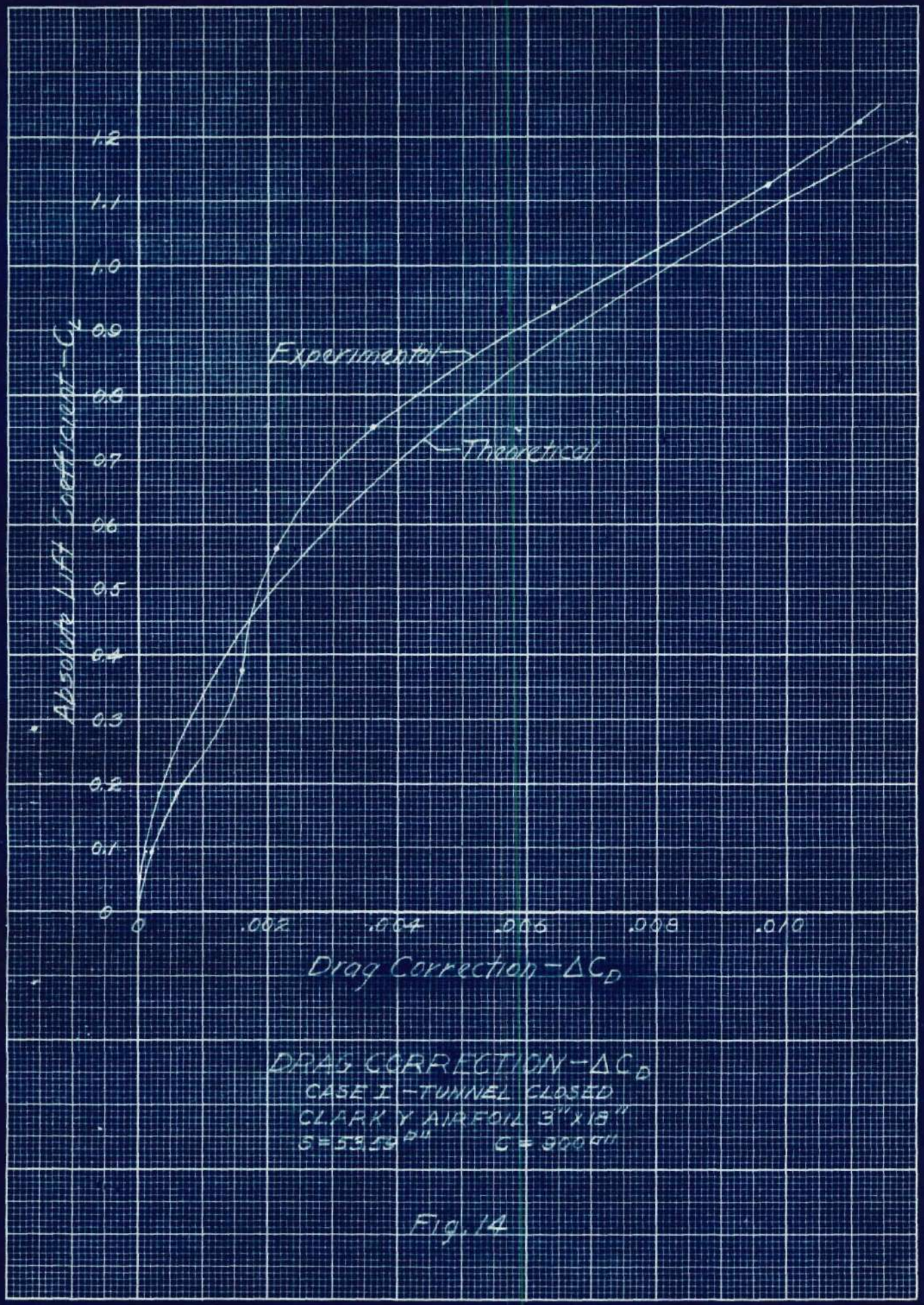

DRAG CORRECTION - ΔC_D
CASE I - TUNNEL CLOSED
CLARK Y AIRFOIL 3" x 18"
S = 53.53 sq in C = 300 sq in

Fig. 14

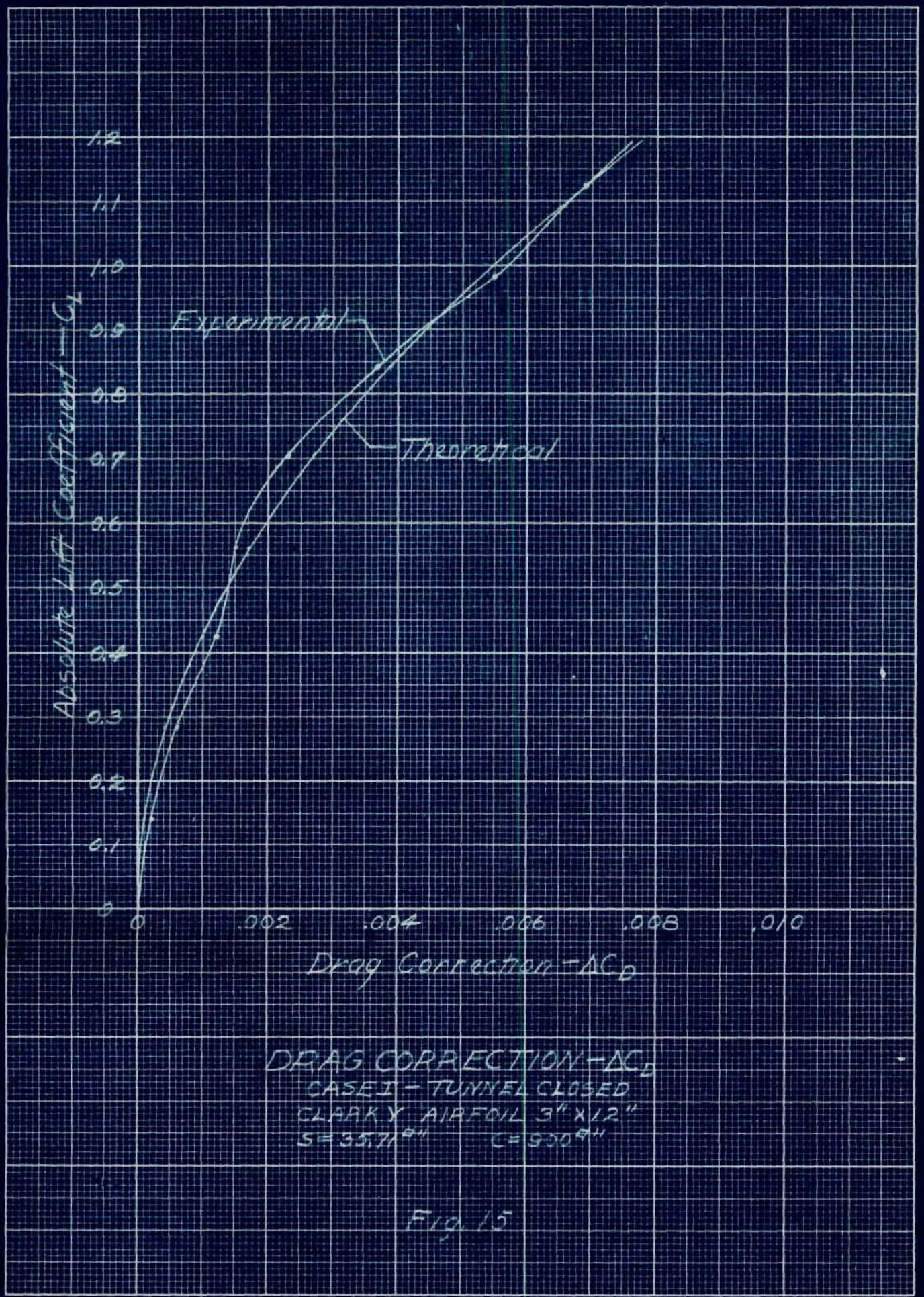

DRAG CORRECTION - ΔC_D
CASE I - TUNNEL CLOSED
CLARK Y AIRFOIL 3" X 12"
S = 35.71 sq in C = 9.50 sq in

Fig. 15

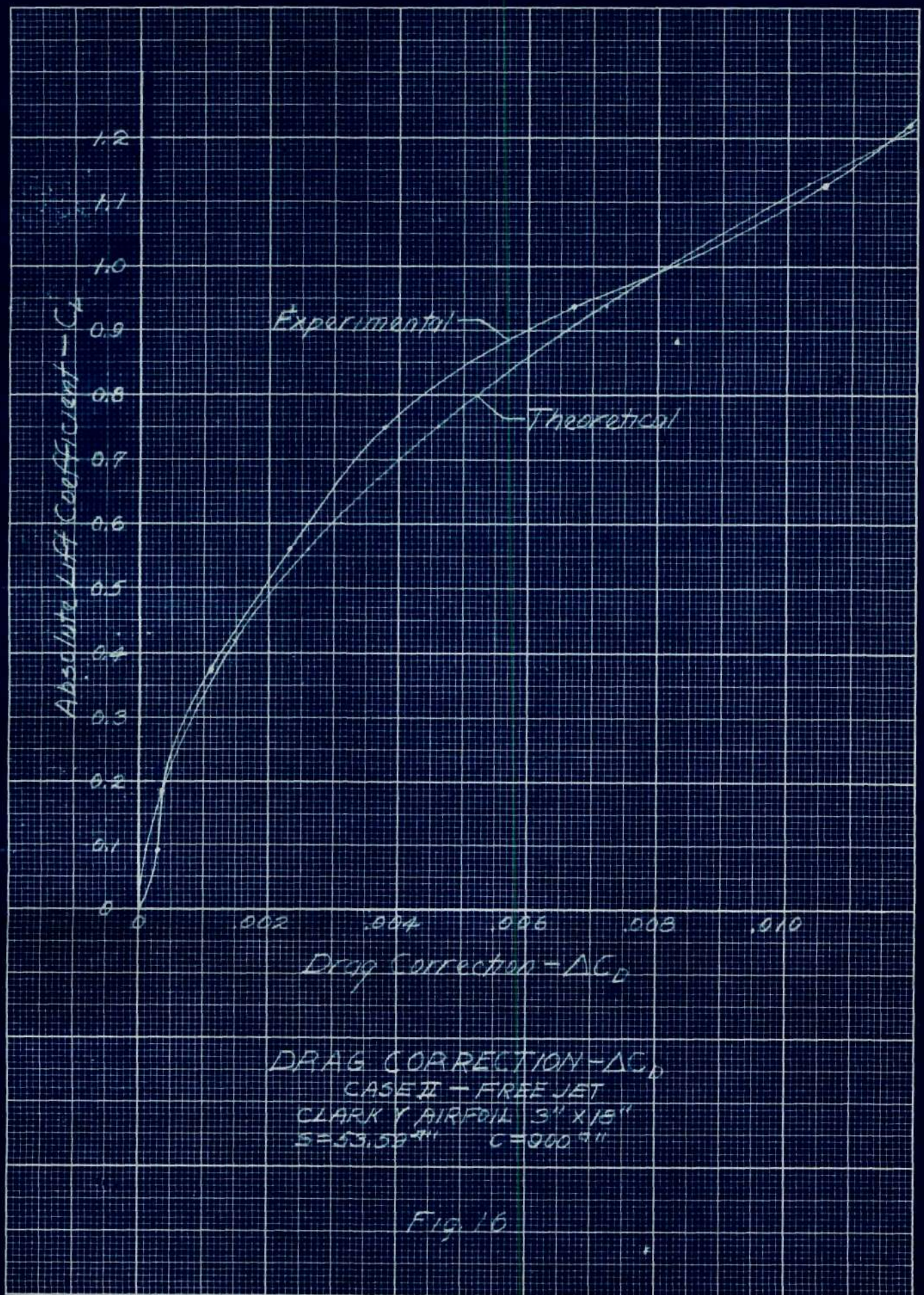

DRAG CORRECTION - ΔC_D
CASE II - FREE JET
CLARK Y AIRFOIL 3" X 15"
S = 53.58 sq in C = 900 sq in

Fig. 16

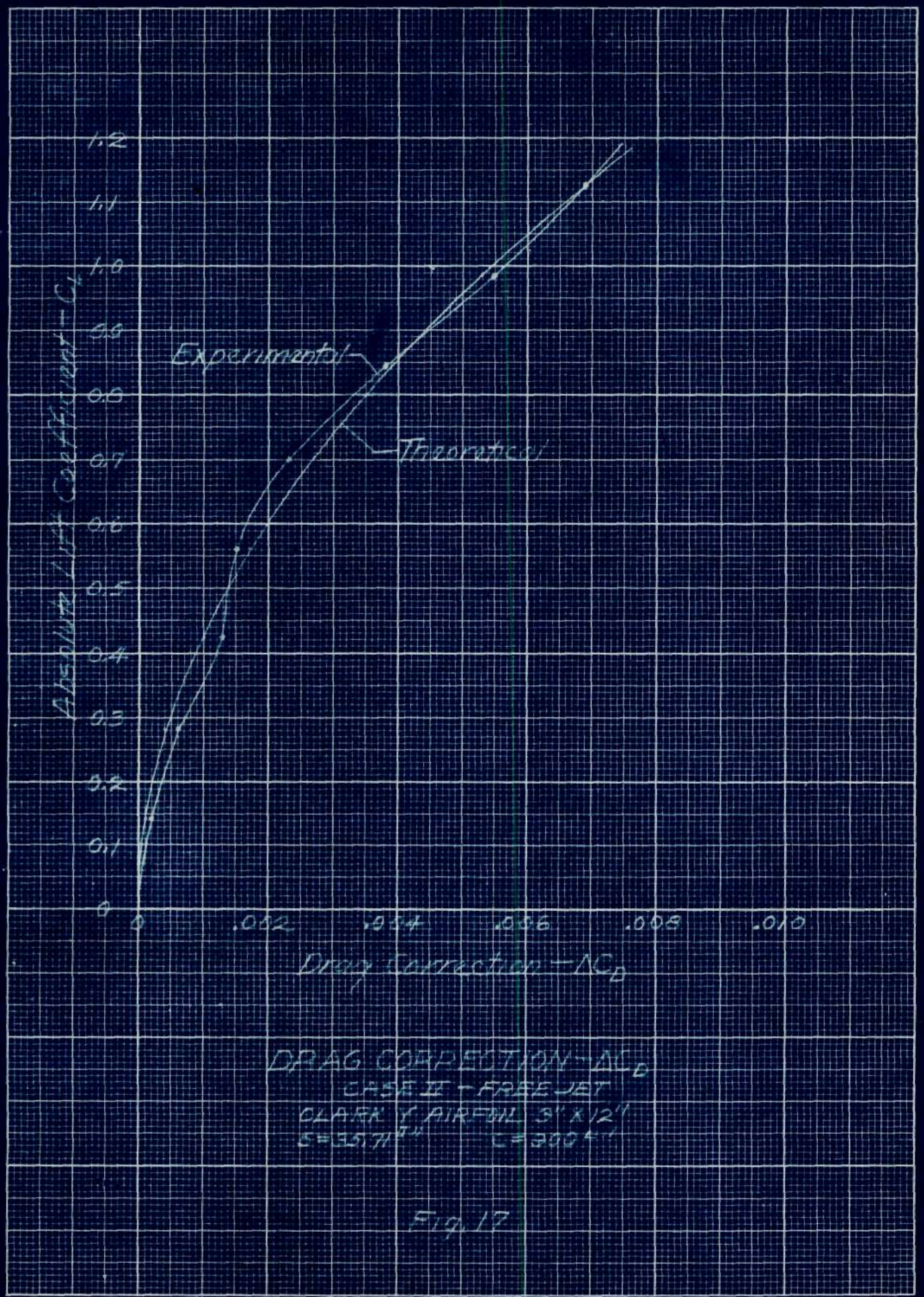

DRAG CORRECTION $-\Delta C_D$
CASE II - FREE JET
CLARK Y AIRFOIL 3" x 12"
S = 35 ft.² L = 200 ft.

Fig. 17

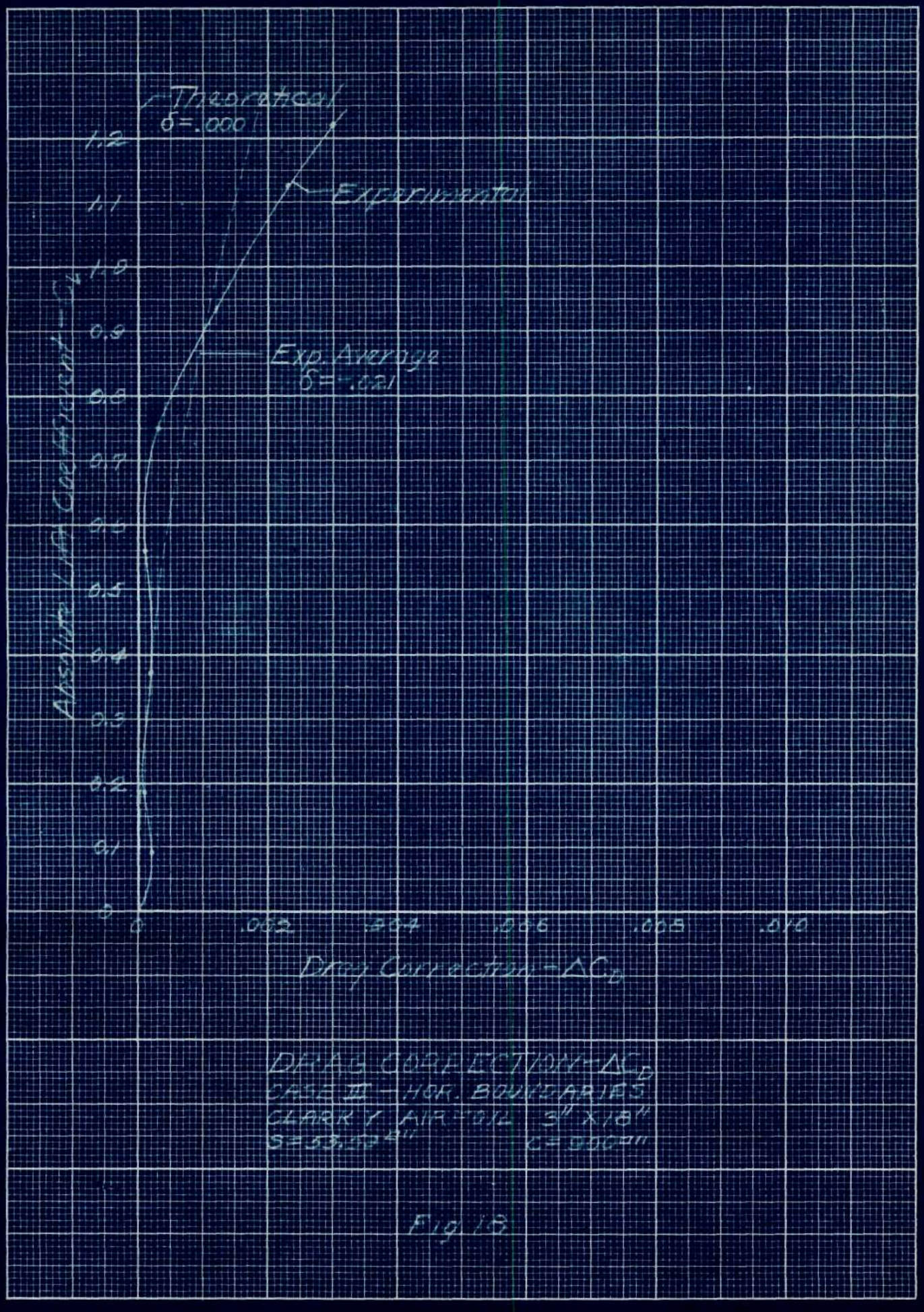

DRAG CORRECTION = ΔC_D
CASE II - HOR. BOUNDARIES
CLARK Y AIRFOIL 3" X 18"
S = 3.5 FT² c = 0.167 FT

Fig 18

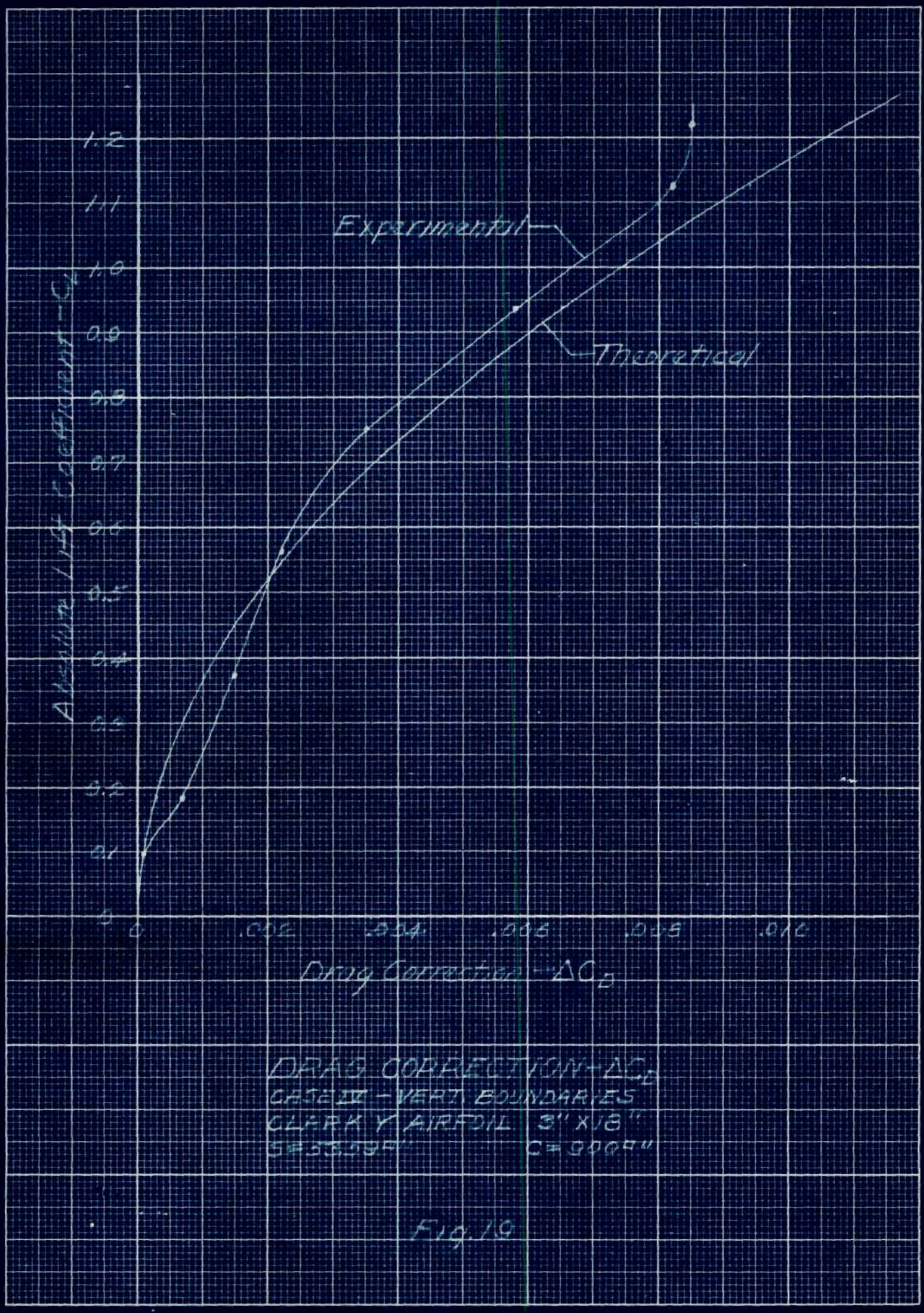

DRAG CORRECTION - ΔC_D
CASE III - VERT. BOUNDARIES
CLARK Y AIRFOIL 3" X 18"
S = 53.59 sq. ft. C = 0.996 ft.

Fig. 10

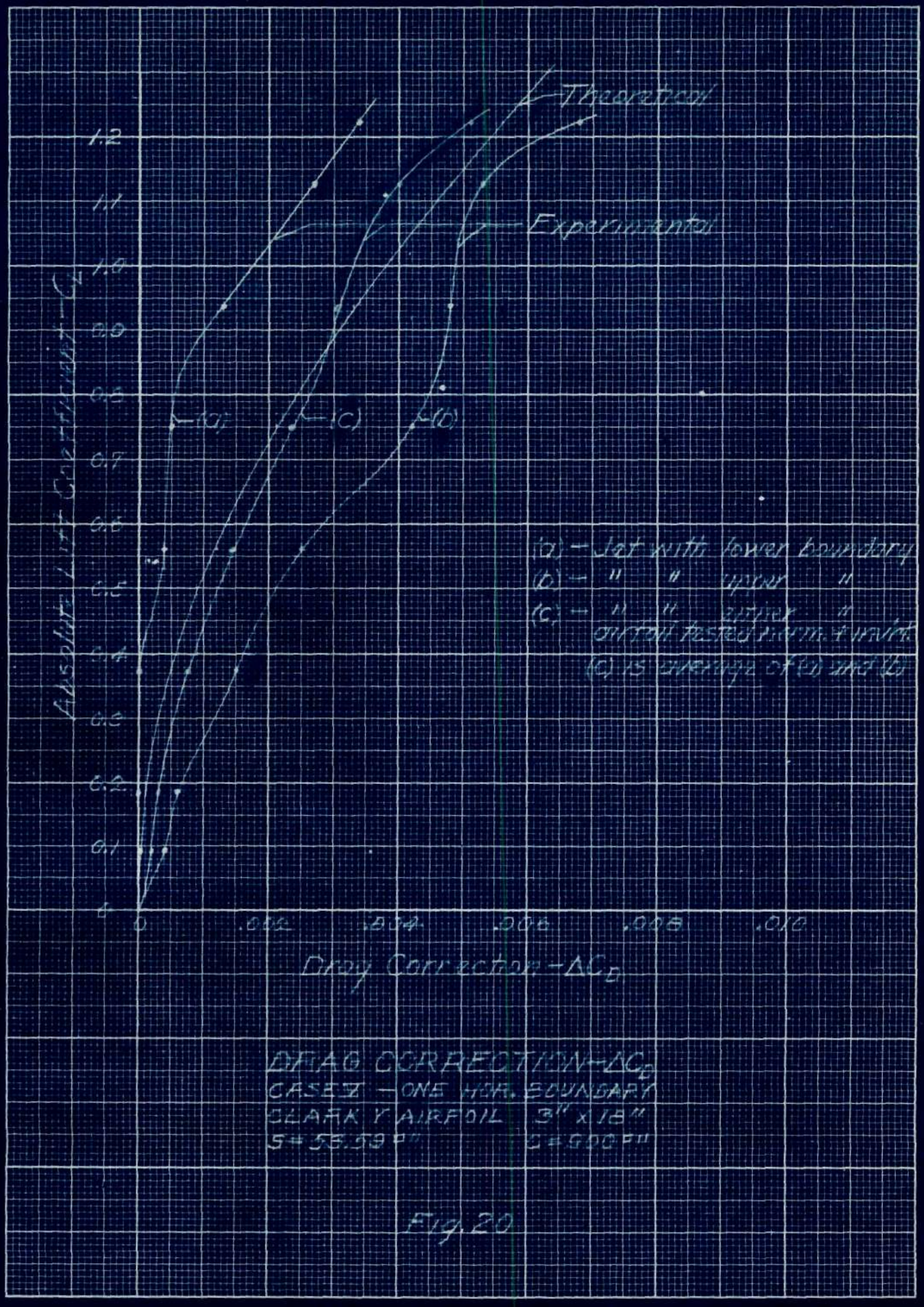

(a) – Jet with lower boundary
(b) – " " upper "
(c) – " " entire " open test section + walls
(c) is average of (a) and (b)

DRAG CORRECTION - ΔC_D
CASE 2 – ONE HOR. BOUNDARY
CLARK Y AIRFOIL 3" x 18"
S = 56.99 sq in C = 600 sq in

Fig. 20

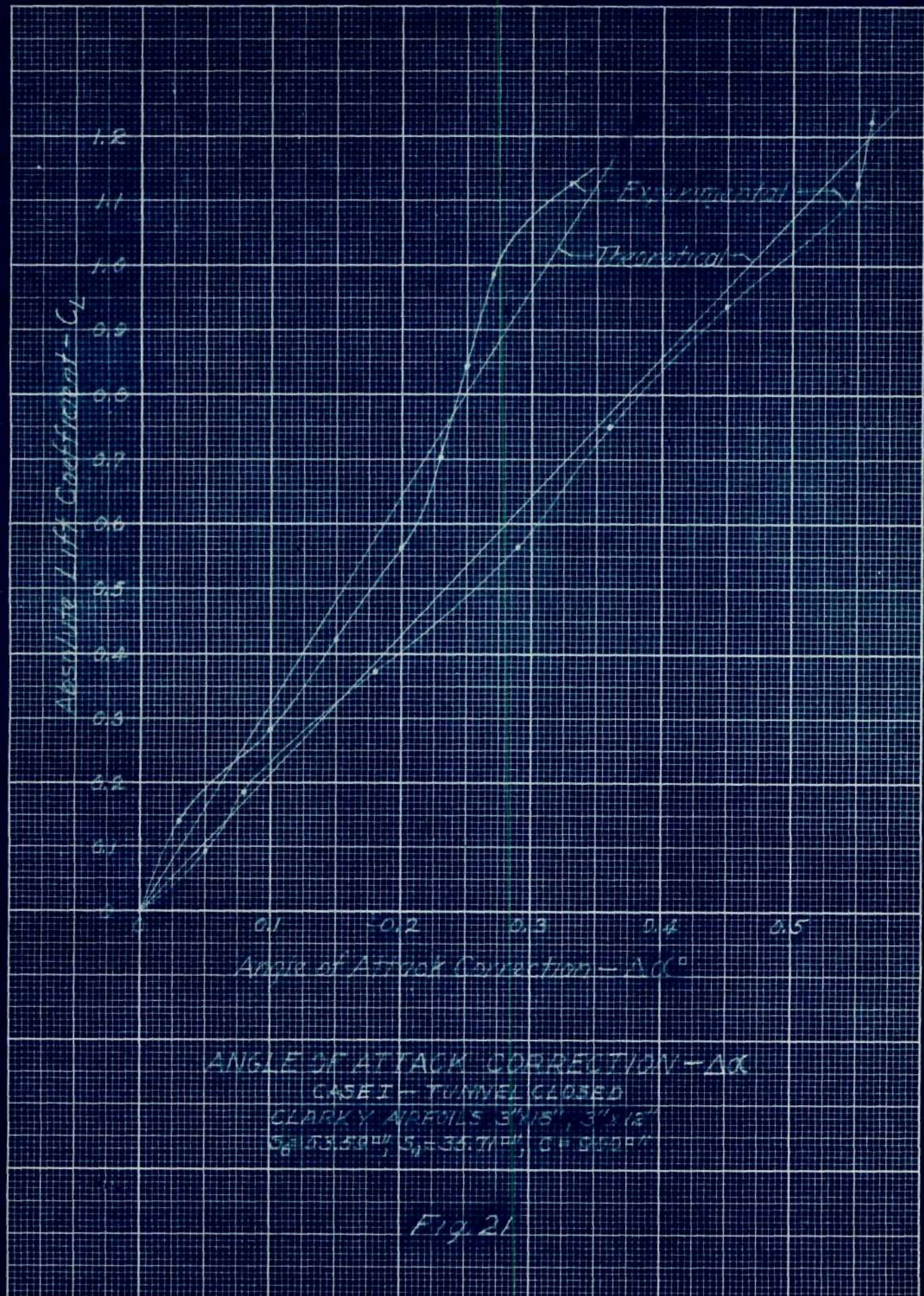

ANGLE OF ATTACK CORRECTION - $\Delta\alpha$

CASE I - TUNNEL CLOSED

CLARK Y AIRFOILS 3" x 15", 3" x 18"

S_B = 25.50 sq. in., S_M = 36.71 sq. in., δ = 0.694

Fig. 21

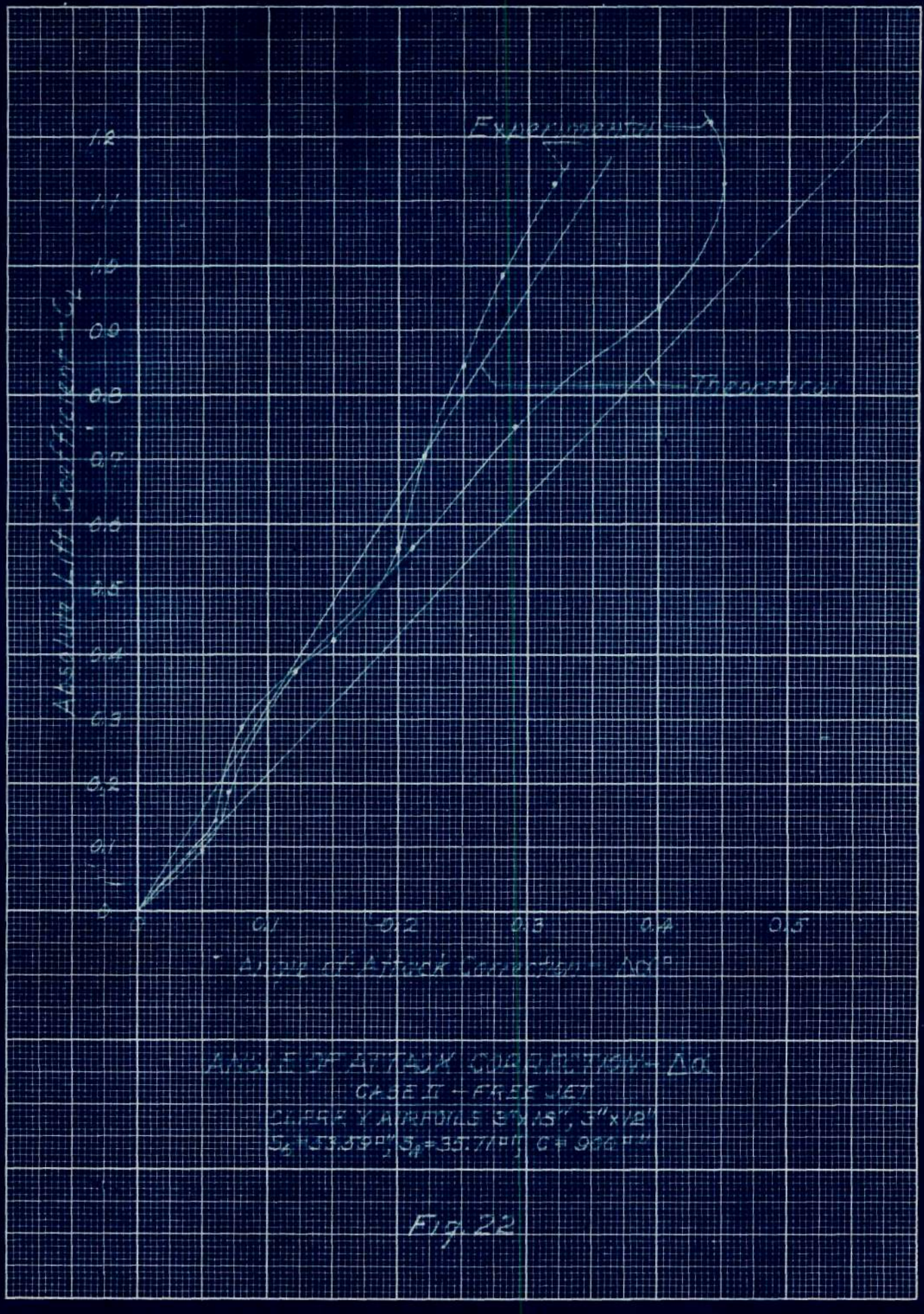

ANGLE OF ATTACK CORRECTION - $\Delta\alpha$

CASE II - FREE JET

CLARK Y AIRFOILS 6" AS", 3" x 12"

S_E = 33.39 ft², S_R = 35.71 ft², C = 0.96 ft

Fig. 22

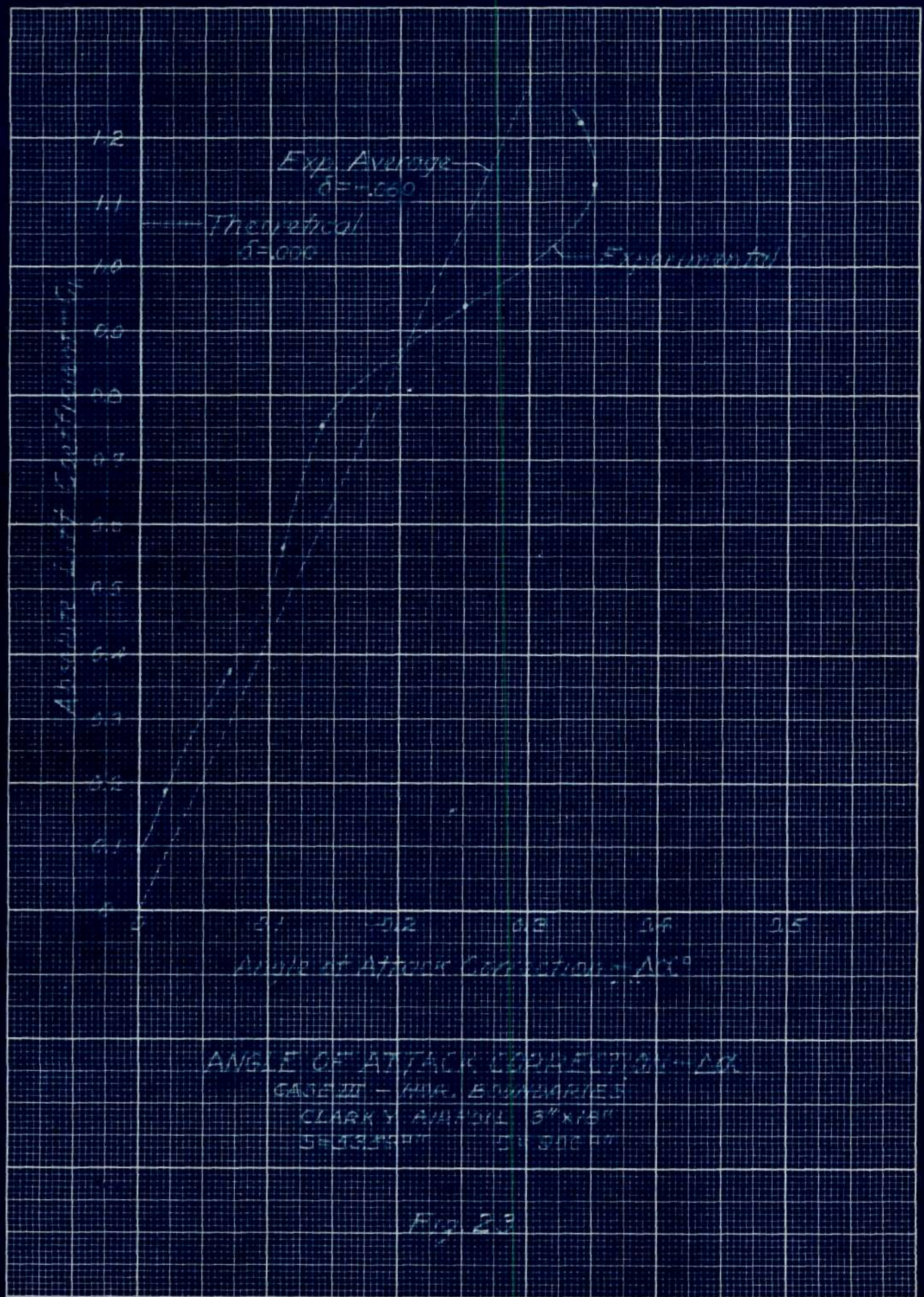

Fig. 23

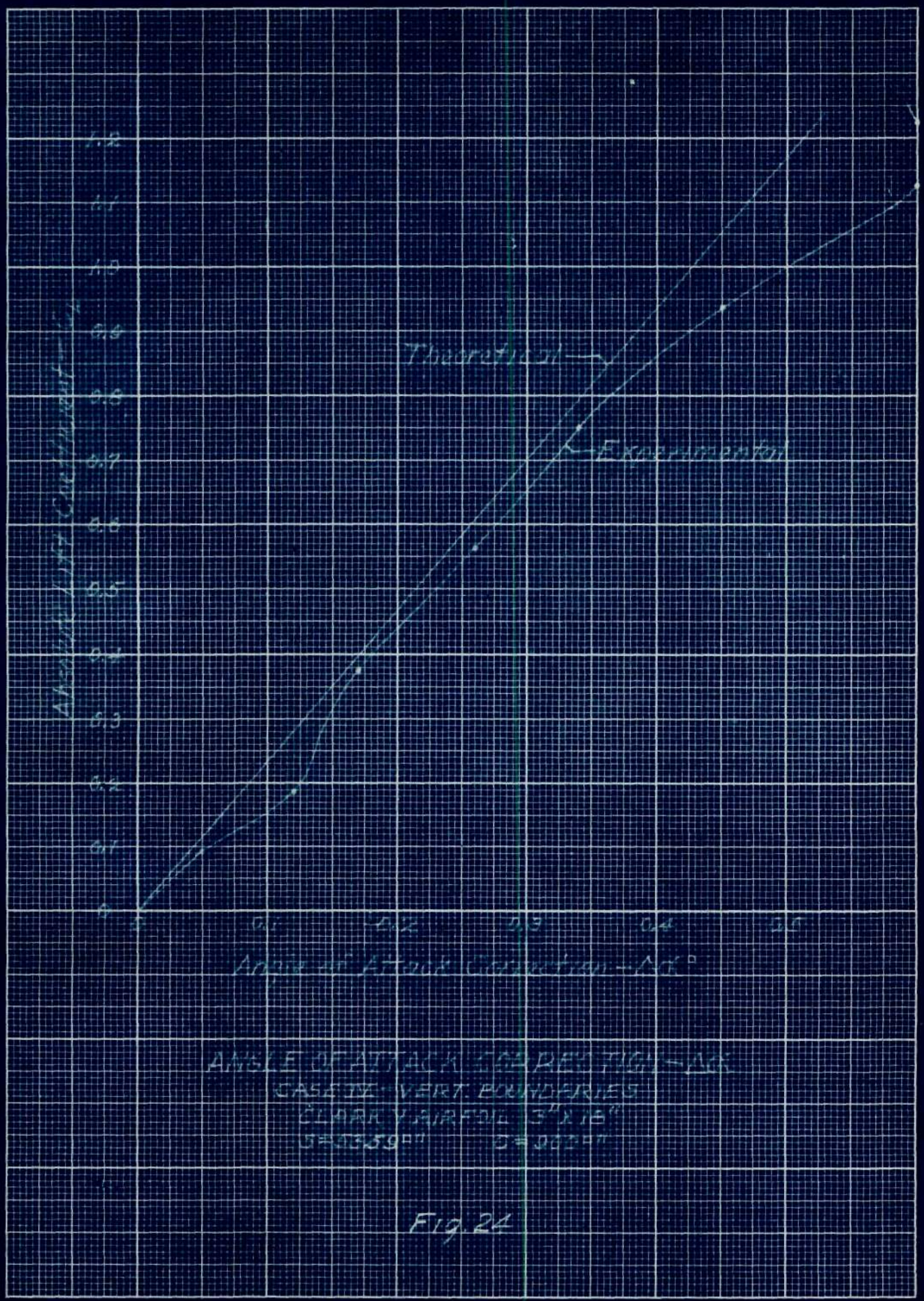

Fig. 24

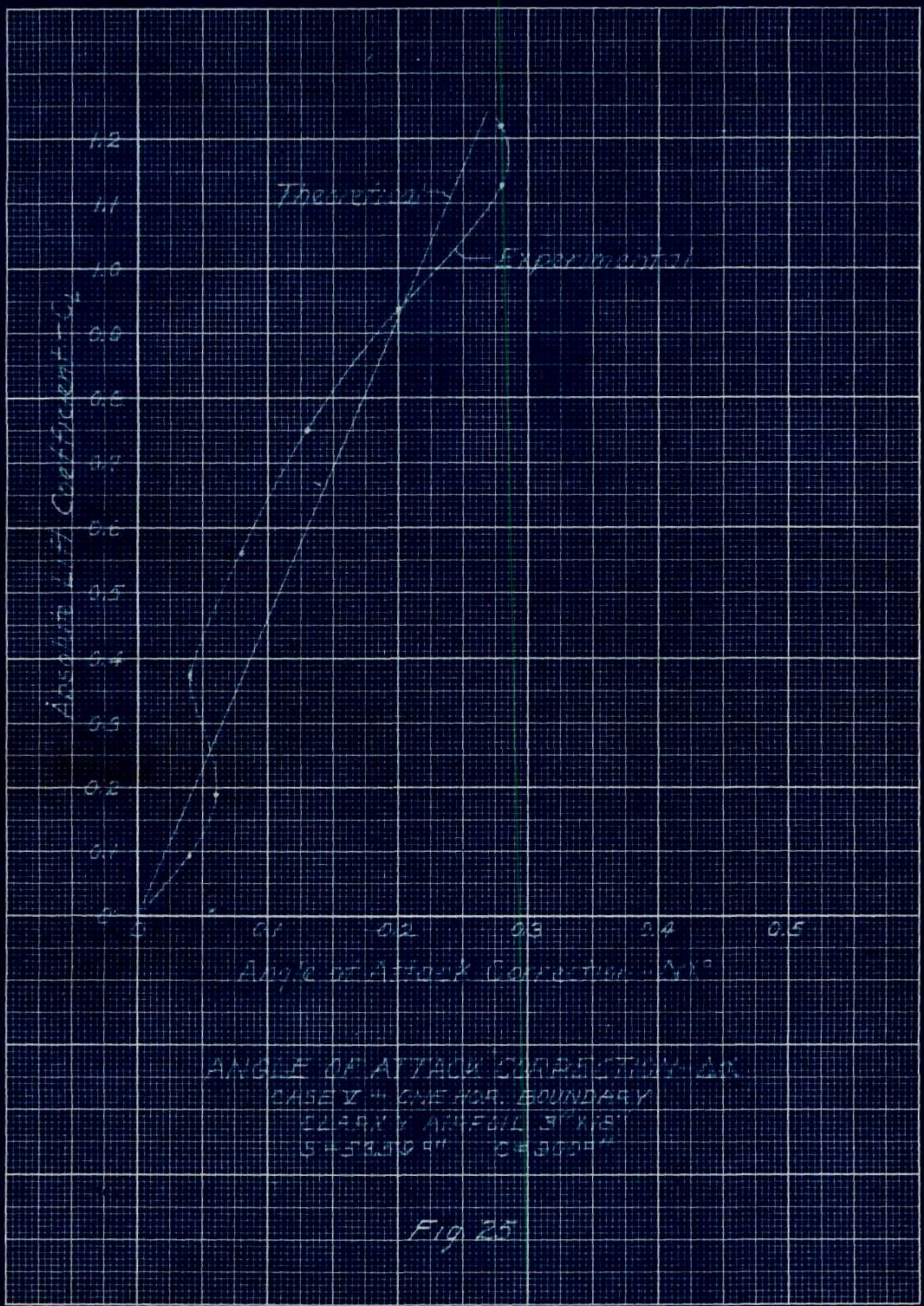

ANGLE OF ATTACK CORRECTION $\Delta\alpha$
CASE V — ONE HOR. BOUNDARY
CLARK Y AIRFOIL $3'' \times 18''$
$S = 54.00$ sq. in. $C = 3.00$ in.

Fig 25